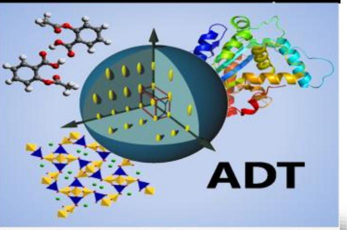

Tomography and Precession Diffraction for 3D Structural Analysis of Nanocrystals

U. Kolb

TU Darmstadt and University of Mainz

kolb@uni-mainz.de

TECHNISCHE UNIVERSITÄT DARMSTADT

JG|U JOHANNES GUTENBERG UNIVERSITÄT MAINZ

Electrons: 10^3 x stronger interaction with matter compared to x-rays

1D – data but probing the bulk

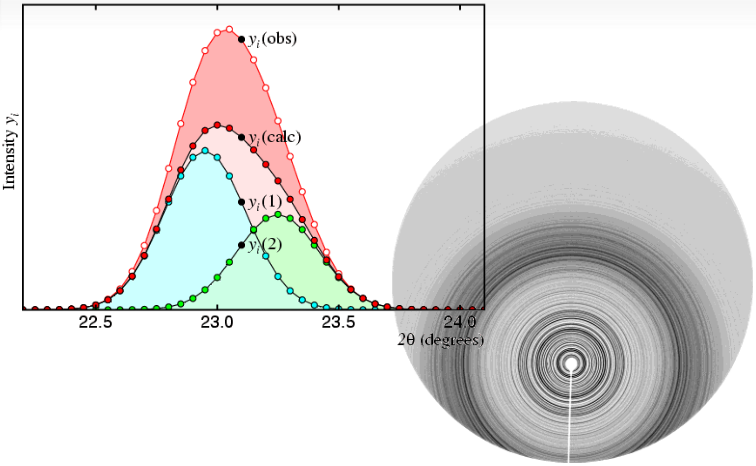

Powder
X-ray diffraction

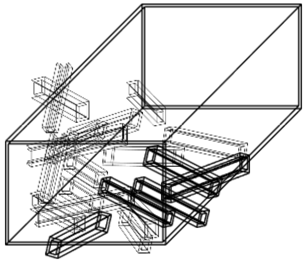

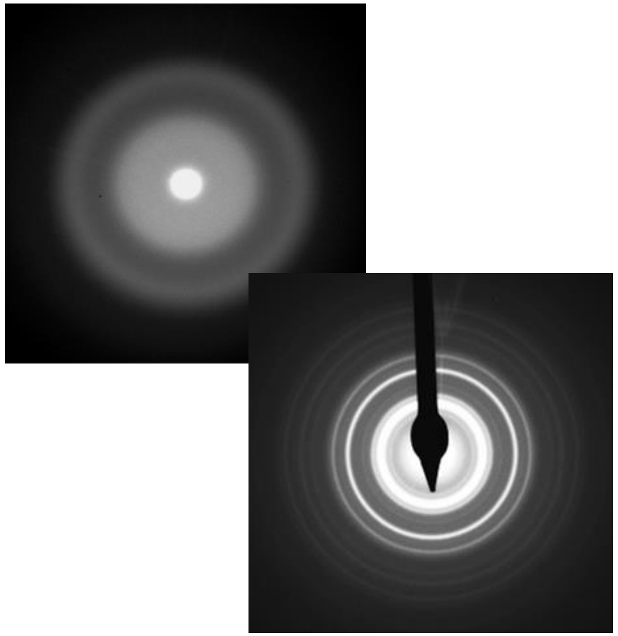

Crystal size

mm

µm

nm

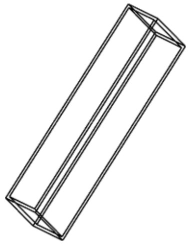

Single crystal
X-ray diffraction

Single crystal
electron diffraction

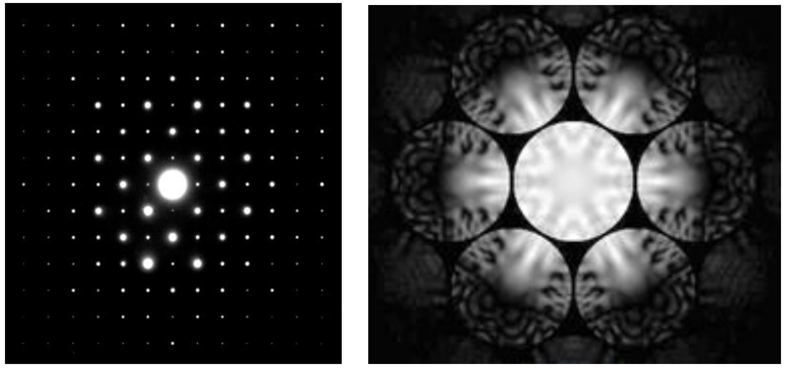

3D – data but limited to the selected crystal

Information available from electron diffraction

- single crystals in polyphasic samples
- phase analysis
- crystal orientation

- cell parameters
- possible space groups
- existence of centrosymmetry
- structure analysis

- superstructures
- twinning
- Stress/strain measurements
- disorder, defects, dislocations

→HRTEM

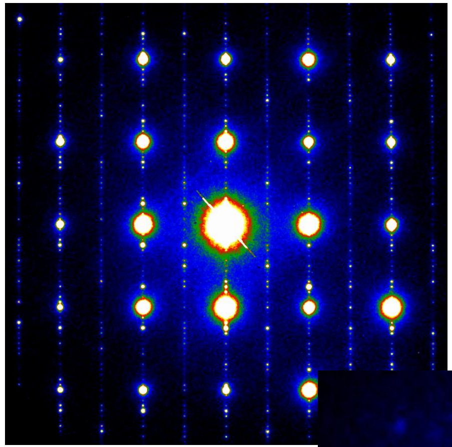

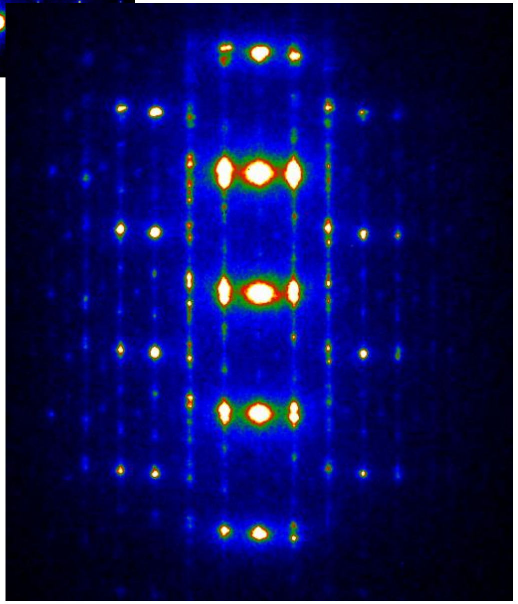

Excitation error s:
crystal cannot be oriented fully
(precision ⟷ radiation damage)

Dynamical scattering:
Strong in oriented zones → wrong intensities, violated extinction rules
CBED: Use of dynamical effects, thick specimens >200 Å

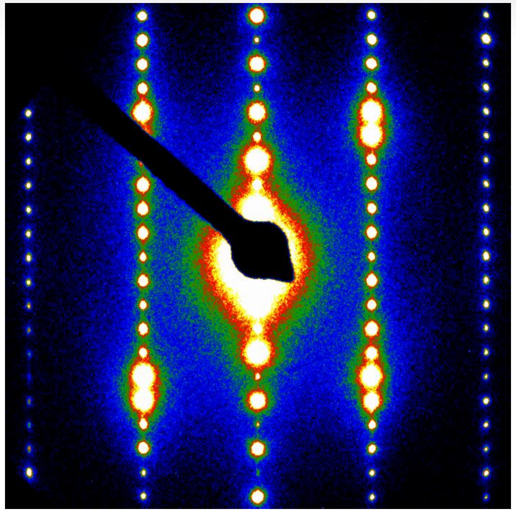

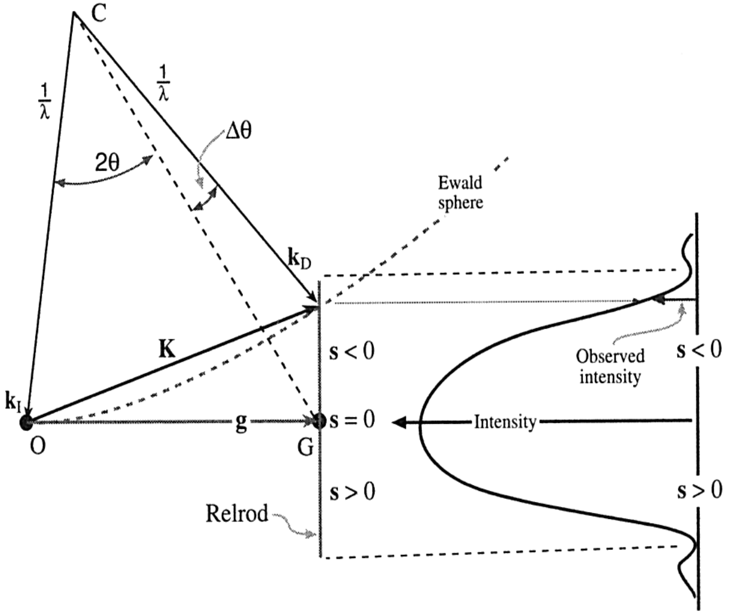

Electron beam precession (Precession electron diffraction PED)

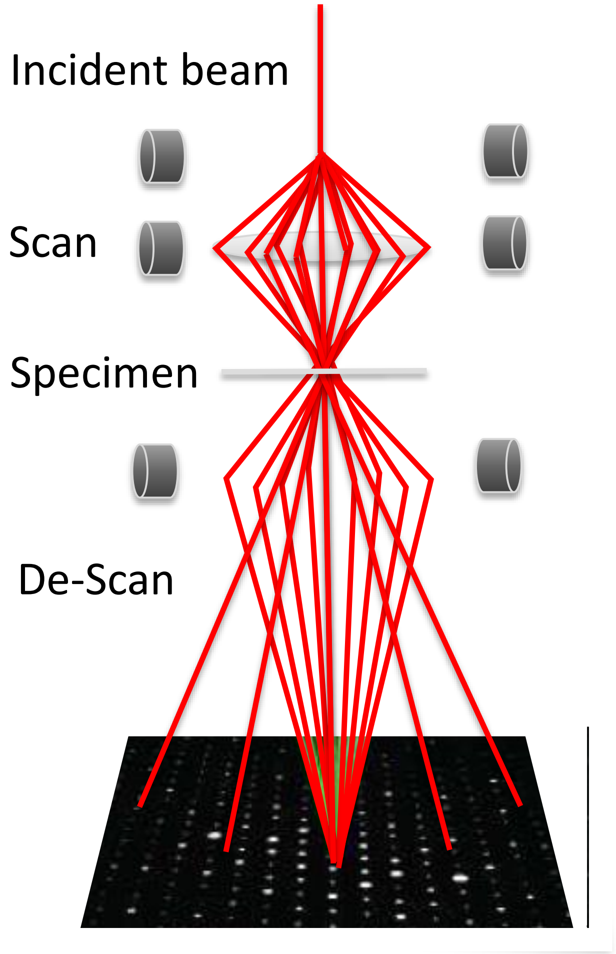

PED:
- One incident beam angle
- Sequentially recorded

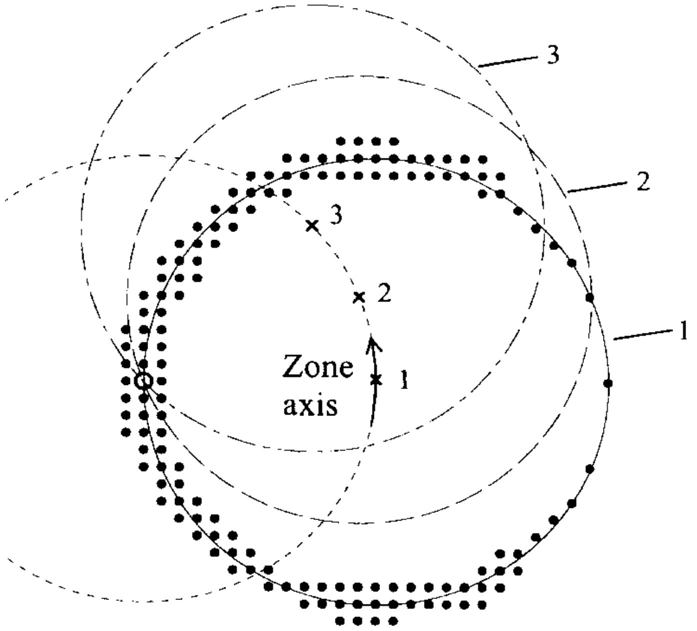

CBED:
- Different incident beam angles
- Simultaneously recorded

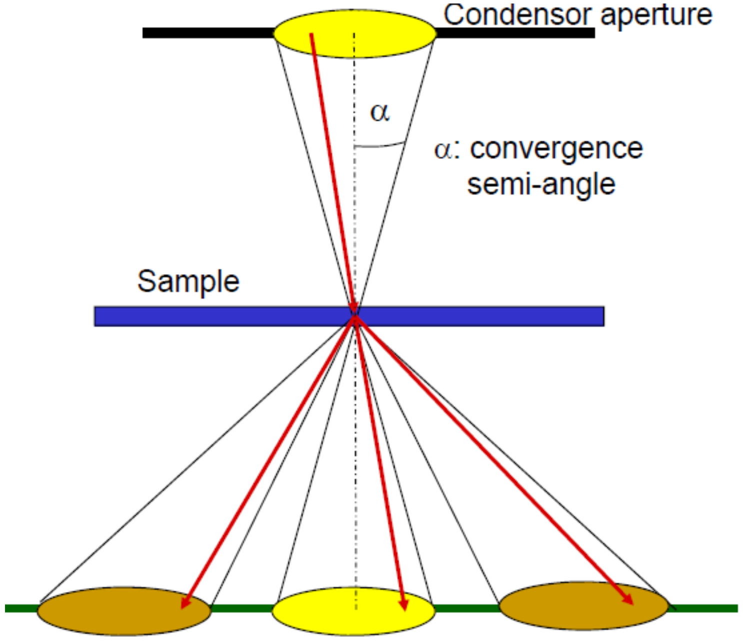

Double conical beam-rocking system for measurement of integrated electron diffraction intensities. R. Vincent, P.A. Midgley, *Ultramicroscopy*, **53**, 271 (1994).

Moving the Ewald sphere: Double diffraction reduction and reflection integration

Double diffraction along systematic row: e.g. (001) and (003) forbidden

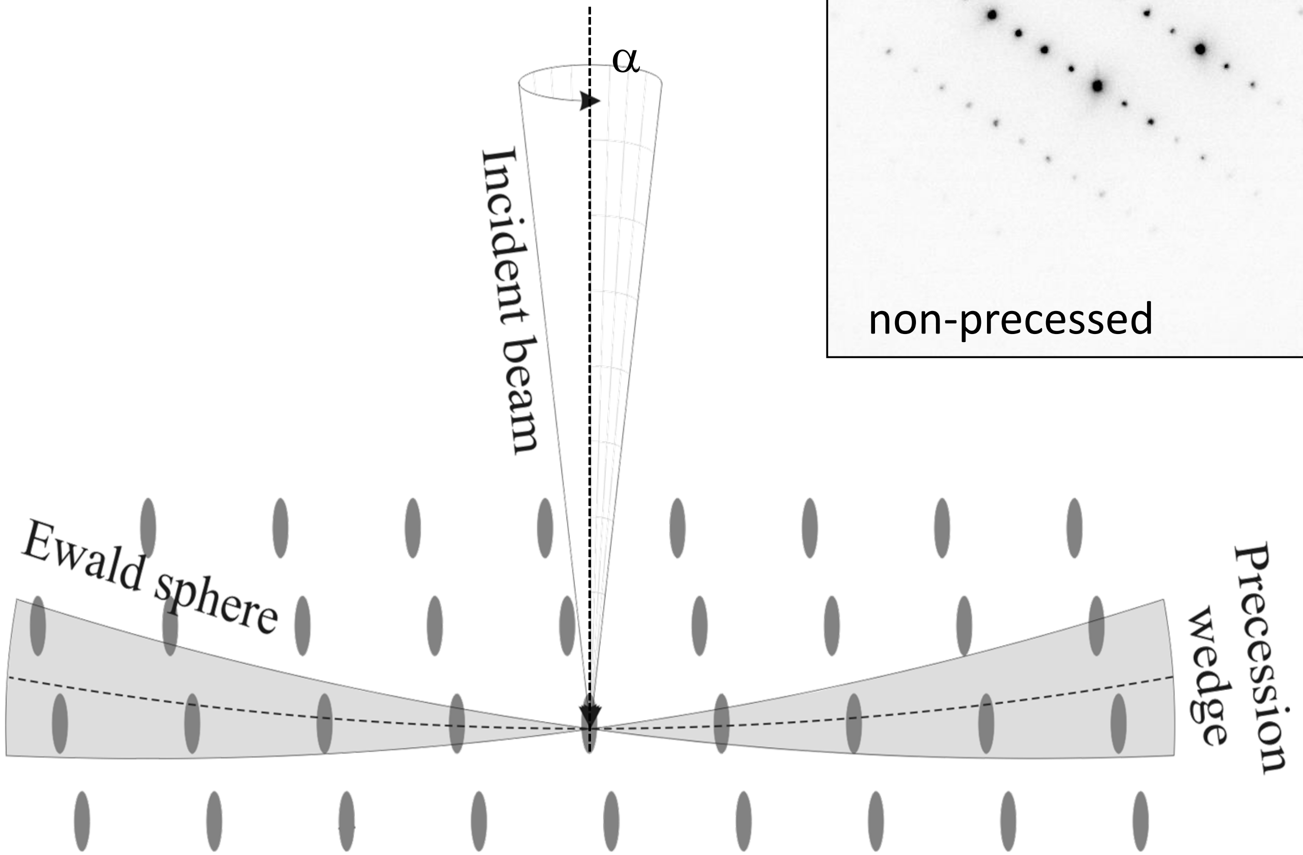

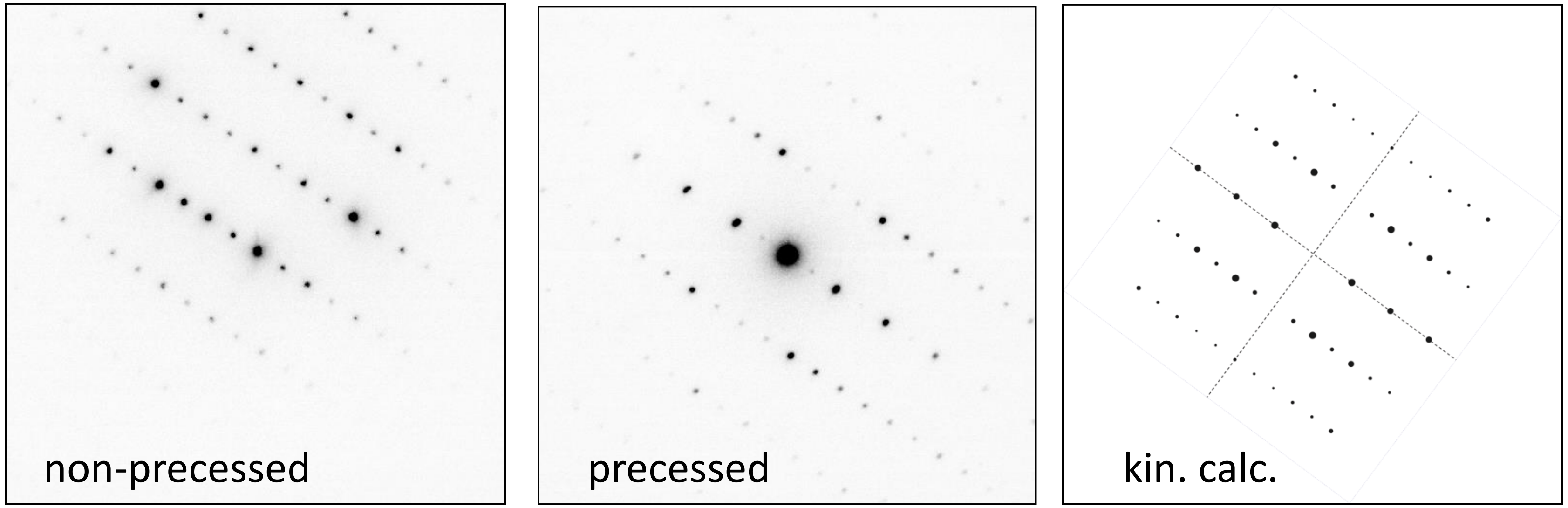

On-Zone

Off-Zone

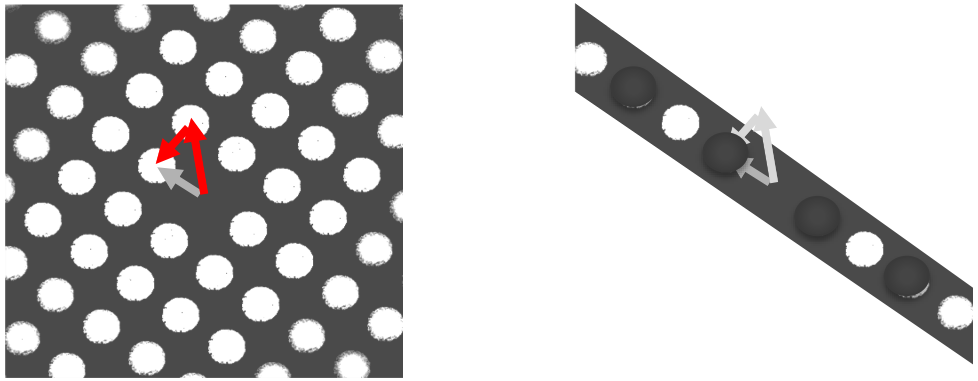

non-precessed

precessed

Measured and (Multislice) simulated precession patterns

Measured and (Multislice) simulated precession patterns (L.D. Marks, Sinklair Northwestern Univ. USA)
Example: Natural Mineral Al_2SiO_5 Orthorhombic Pnnm with 32 atoms/unit cell (Andalusite)

Bragg's Law Simulation

Experimental
Multislice

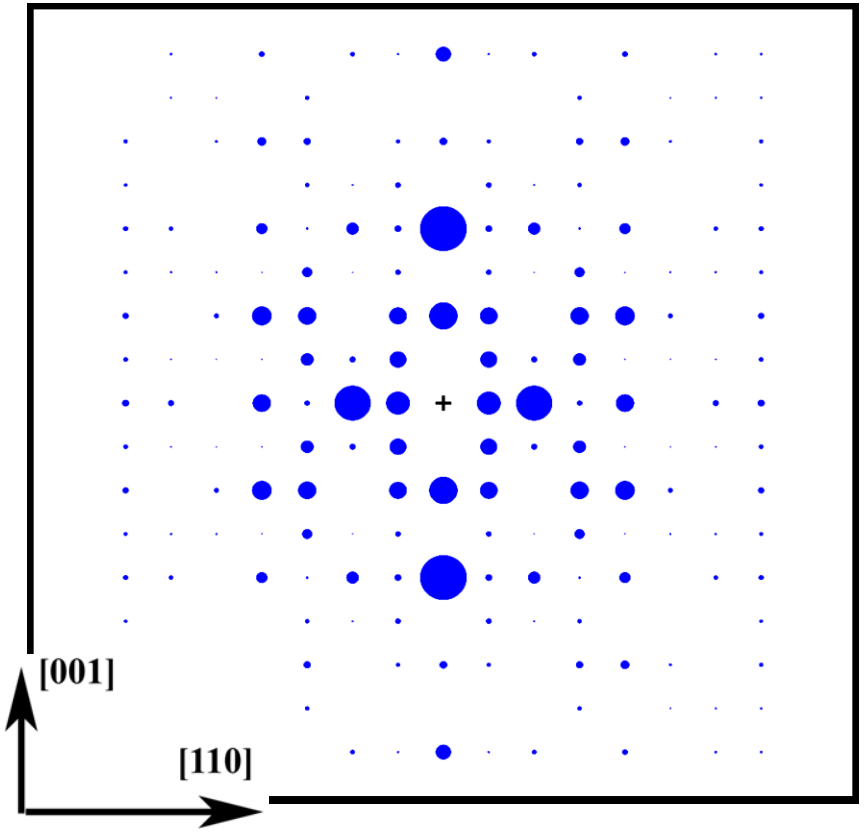

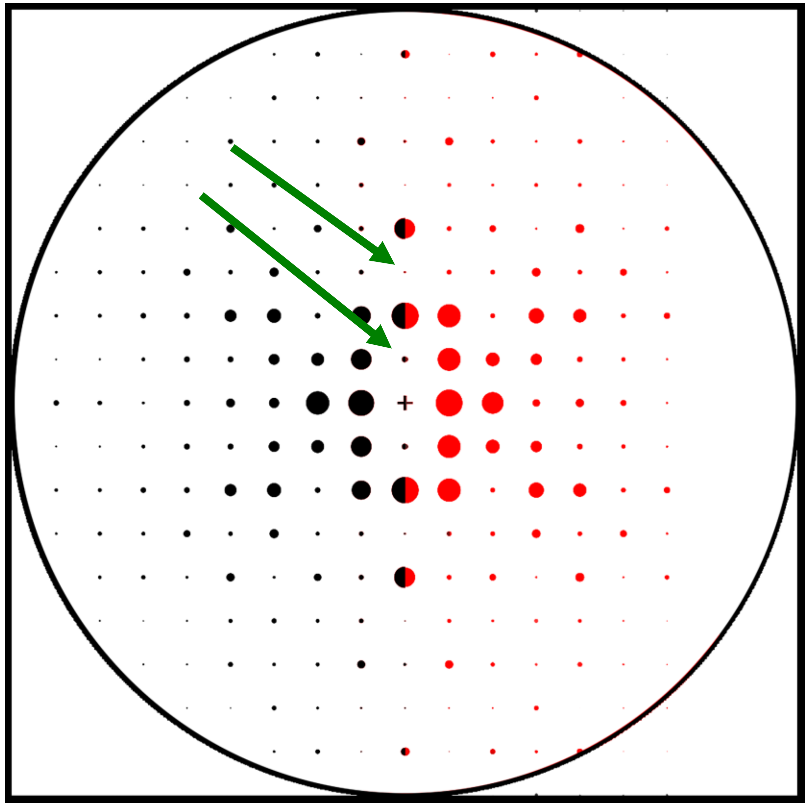

32 mrad

With increasing precession angle:
Exponential decay of forbidden reflections

Linear decay of e.g. non-forbidden (002) reflection

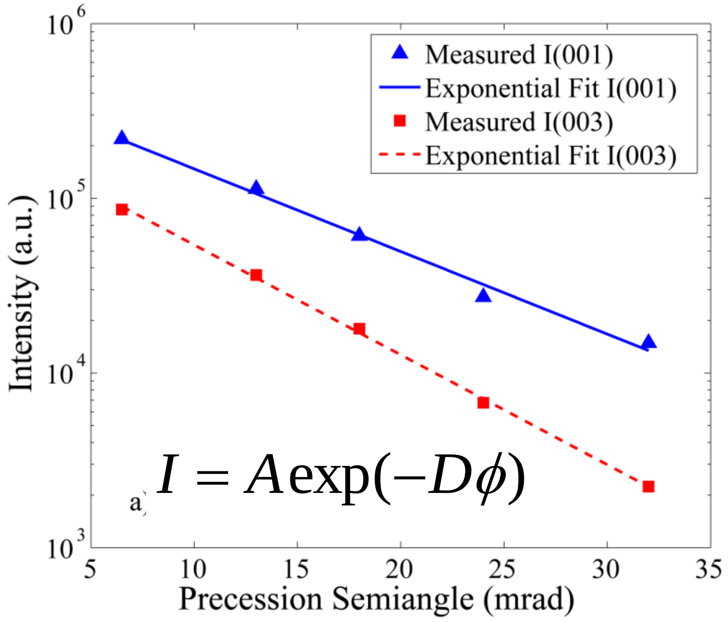

Rate of decay is relatively invariant of the crystal thickness

Courtesy L.D. Marks,

Precession diffraction angle

- increase of the number of diffraction spots intercepted by the Ewald sphere
- integration over the reflection intensity and reduction of the excitation error effect
- reducing the effect of slight misorientation of the sample
- reduction of the dynamical effects and the diffraction dependency on the thickness of the sample

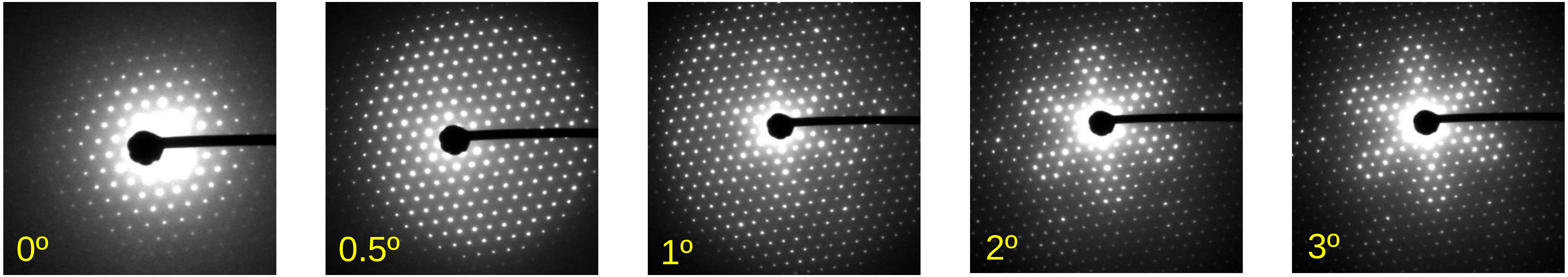

Increasing precession angle → increasing resolution in diffraction pattern (i.e. more diffraction spots are seen).

Example: Mayenite [111] $Ca_{12}Al_{14}O_{33}$ Space group: *I43d*

Selected Area Electron Diffraction (SAED) or Nano Electron Diffraction (NED) or (NBD)

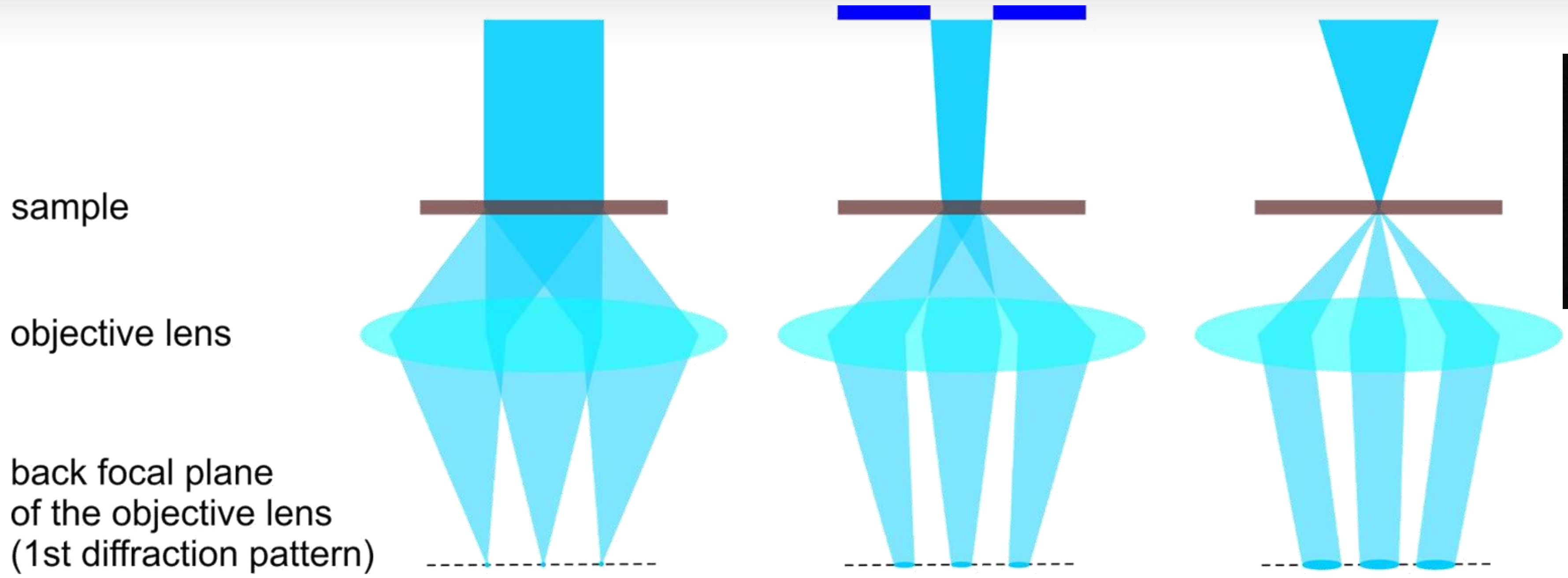

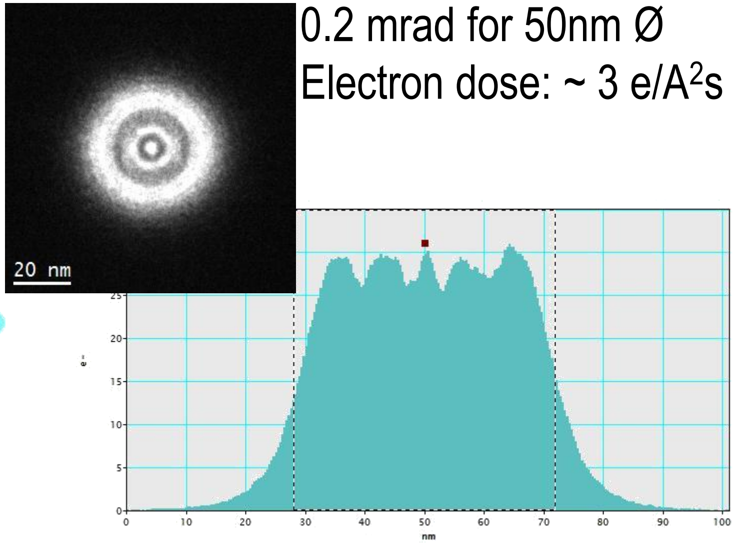

Convergence angle:
0.2 mrad for 50nm Ø
Electron dose: ~ 3 e/A^{2}s

Advantages of nanodiffraction

- free control over the beam size
- we do not unnecessarily damage the sample
- possible to move the beam over the crystal
- we are sure about the area we are collecting the information from

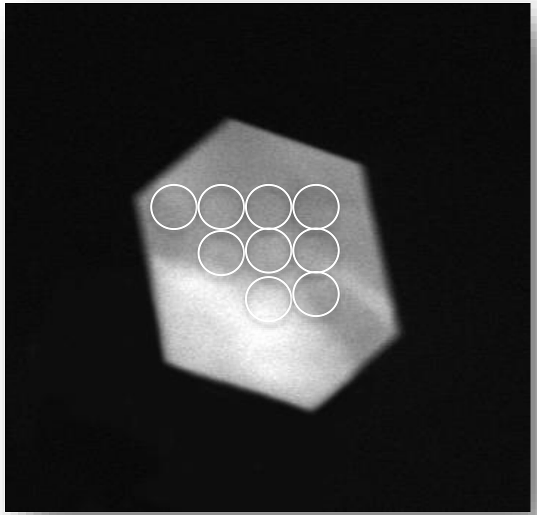

A-Star Acquisition

Acquisition of precession electron diffraction spot patterns

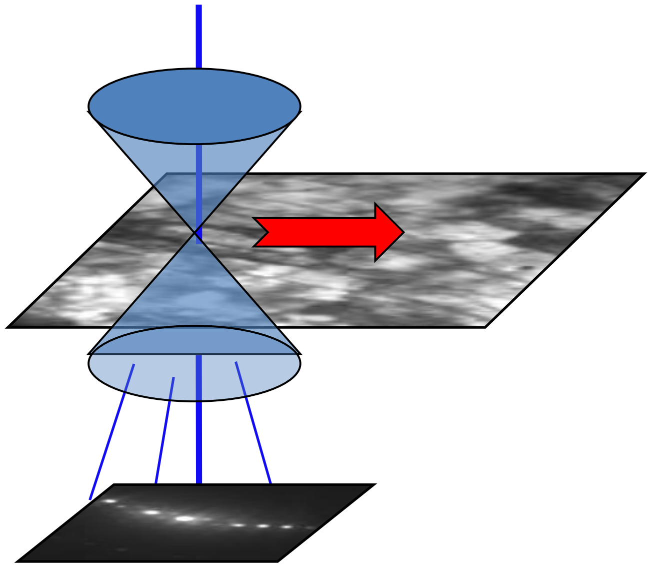

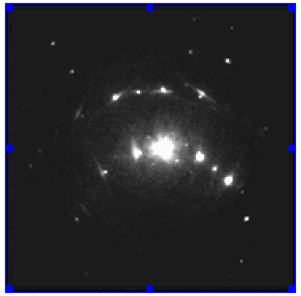

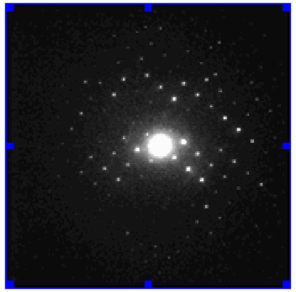

Non-precessed **precessed**

Orientation map

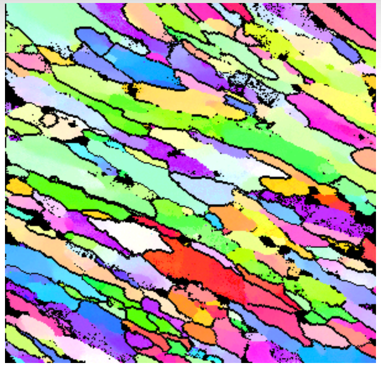

Pt particles, Prof. P. Ferreira, J. Ganesh Univ Texas at Austin USA JEOL 2010 FEG (1 nm resolution)

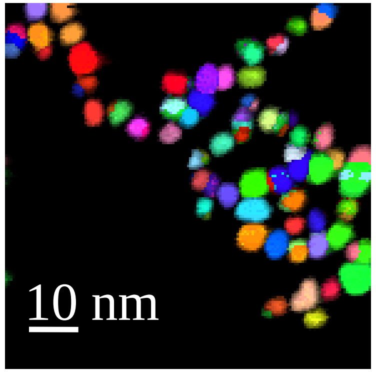

Phase map

Mg-Cu-Gd partly recrystallized metallic glass with Mg_2Cu and Cu_2Gd crystalline precipitates

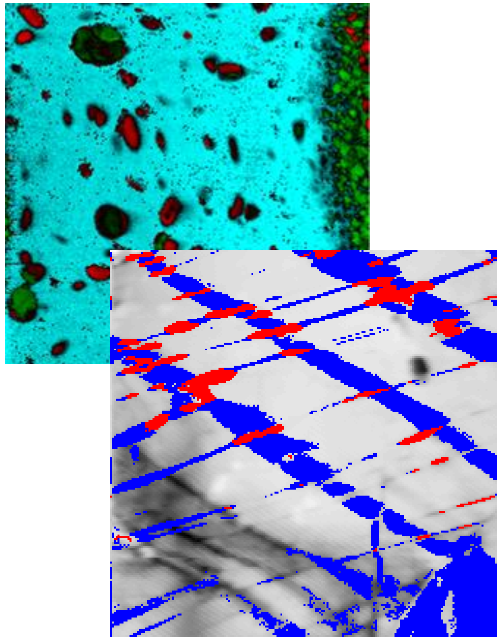

Strain map

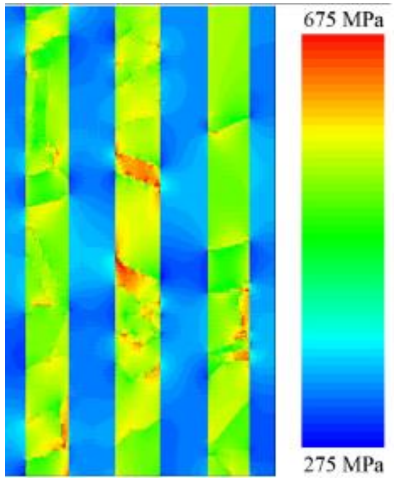

Rhee, Y. Du, P. S. Ho, Journal of Applied Physics, ***93*** *(2003) 3926*

Crystallographic Orientation and Phase Identification

Template generation using Diffgen of all possible simulated orientations (every1º) within stereographic triangle for given crystal lattice(s) and symmetry

Pre-calculated templates

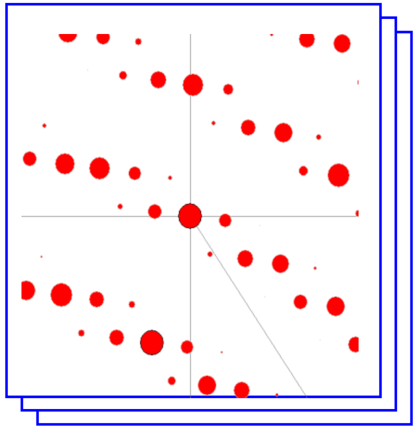

$$Q(i) \sim \sum_{j=1}^{m} P(x_j,y_j)\, T_i(x_j,y_j)$$

Correlation index

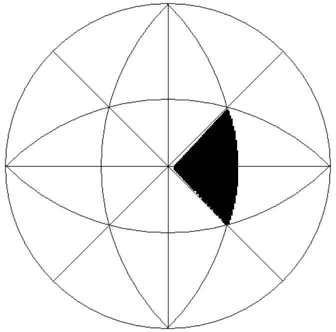

Acquired pattern

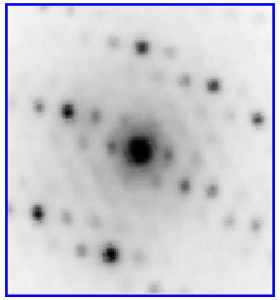

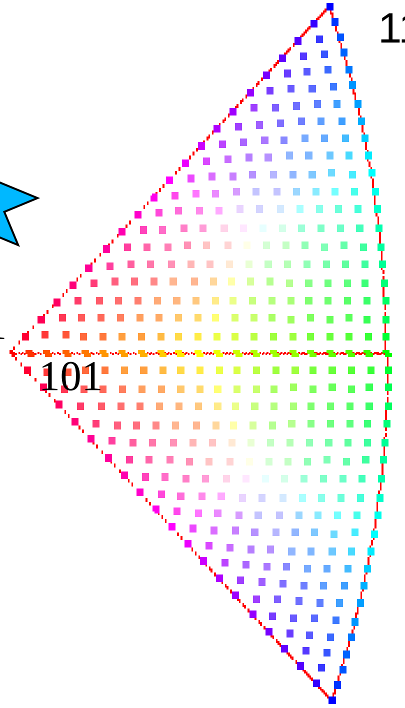

Stereographic projection

(example ,cubic)

~ 2000 simulated patterns

Degree of matching between experimental patterns and simulated templates is given by a correlation index ; highest value corresponds to the adequate orientation/phase

Identification example: nanocrystalline Cu

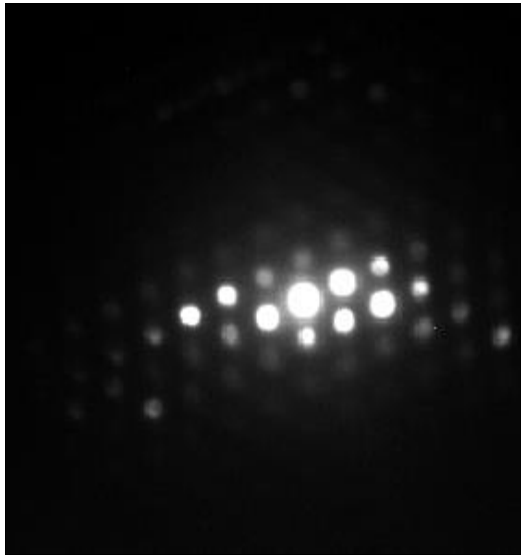

Diffraction pattern

(nanocrystalline cubic copper)

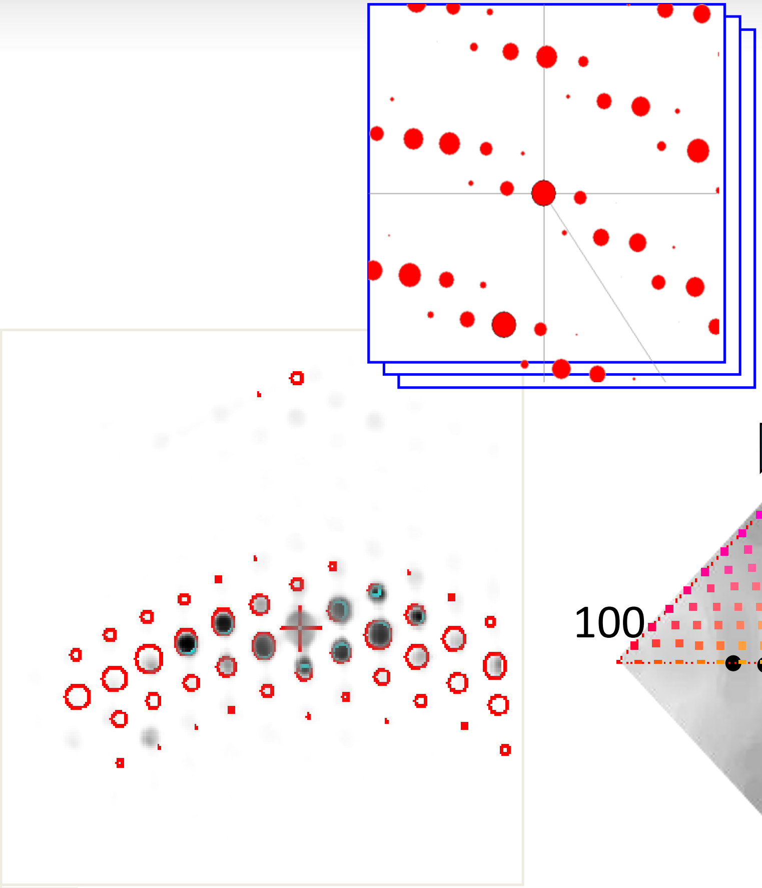

correlation index = 585

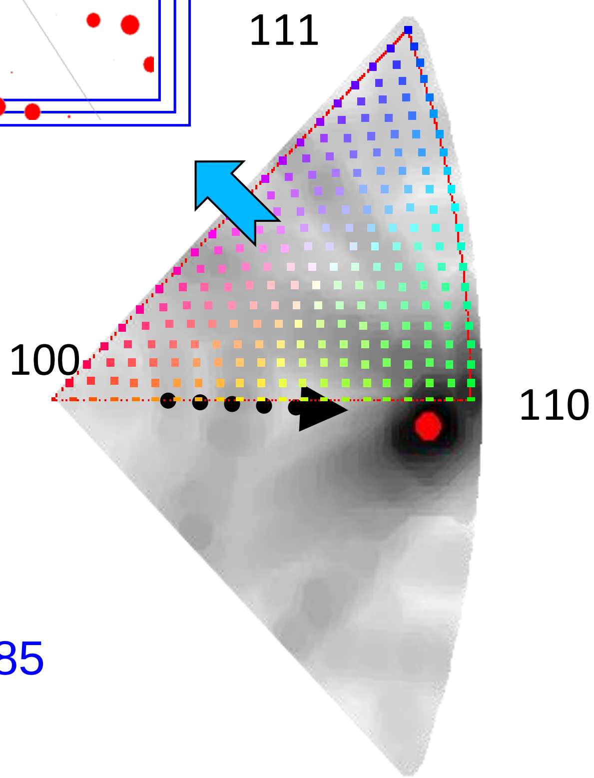

Correlation index map

250 x 200 pixel data acquisition: ~ 5 min
Typical software data analysis time
cubic: 5-15 min
hexagonal , tetragonal: x 3- 4 more time

Orientation map of severely deformed copper

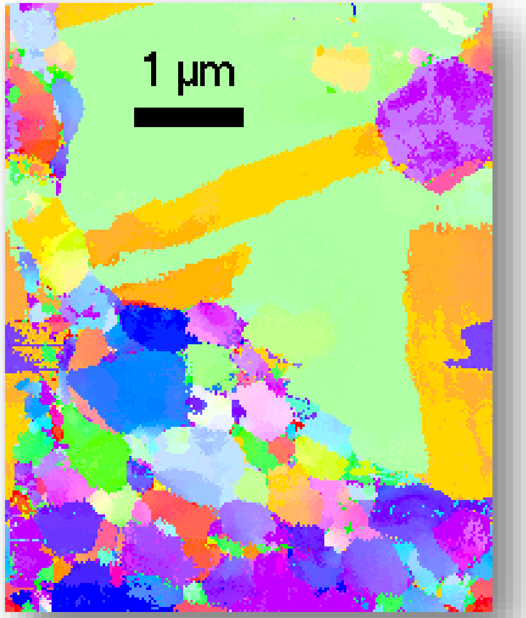

NBD step 20 nm

NanoMEGAS Advanced Tools for electron diffraction

Grenoble INP

Different microscopes

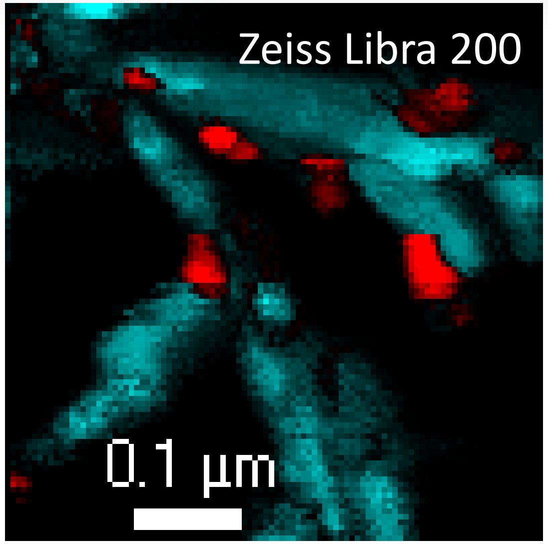

M. Gemmi, IIT Pisa

0.3° precession

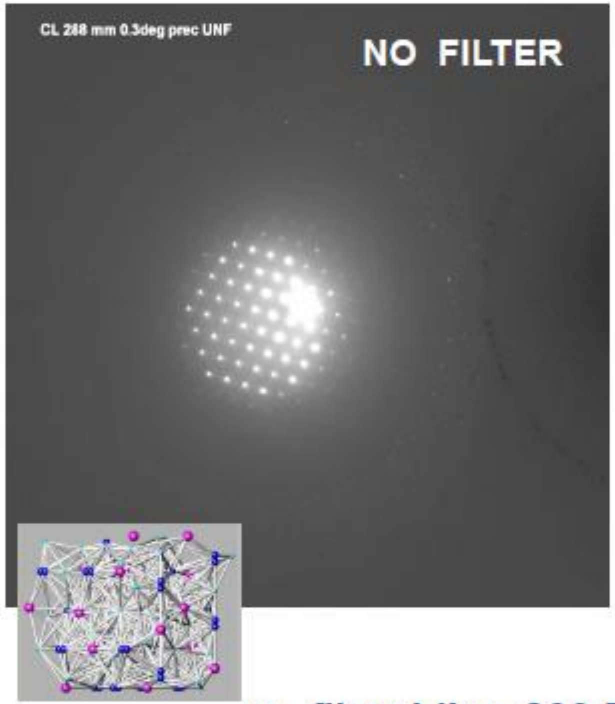

0.3° precession

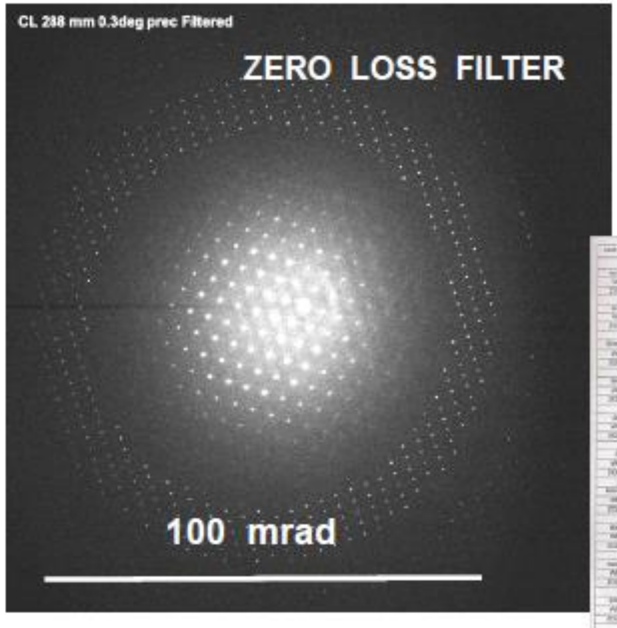

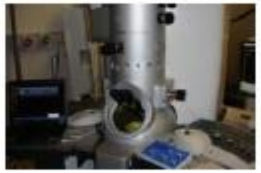

Mornirolli et al

Ω filter Libra 200 FE : 100 mrad acceptance angle (ΔE = 10 eV)

➡ more information

➡ *visualize precisely high order/resolution reflections*

NanoMEGAS
Advanced Tools for electron diffraction

Drug Delivery applications & Texture of nanoparticles

Unpublished results Courtesy of M Gemmi IIT Pisa Italy.

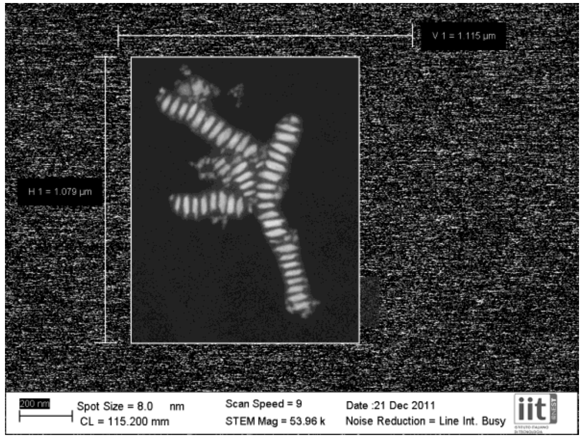

Orientation mapping with 10nm resolution

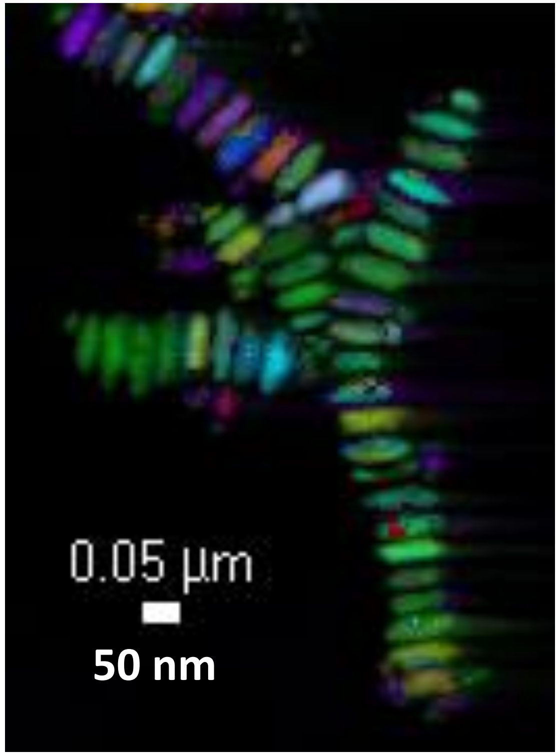

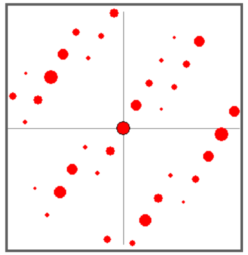

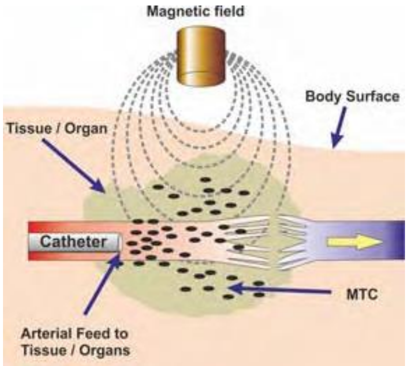

Matching of each collected pattern with a generated data bank

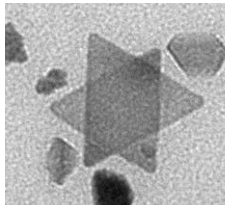

1 Fe3O4 nanoparticle (vertical view)

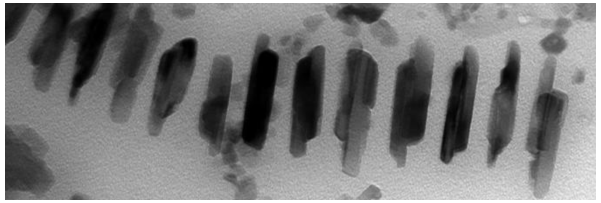

Several Fe3O4 nanoparticles self assembeld (lateral view)

ISTITUTO ITALIANO DI TECNOLOGIA

Nanoparticle (50 nm) phase identification

Nanoparticle (50 nm) phase identification

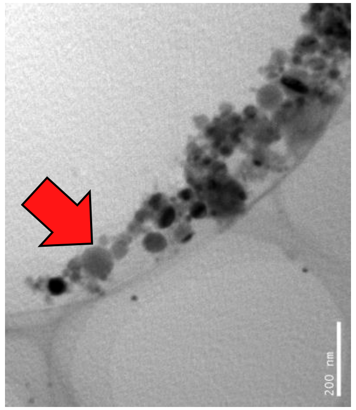

cubic 8.32 A

$Fd\bar{3}m$

Magnetite or maghemite ??

$P4_132$ **γ-Fe_2O_3**

Fe_3O_4

cubic 8.32 A

Orientation map precession 0.3º

PHASE map precession 0.3º

ALL Nanoparticles

REVEALED AS

magnetite (RED)

NanoMEGAS Advanced Tools for electron diffraction

Grenoble INP

INDEX and create virtual dark and bright field maps

Diffraction Pattern viewer with virtual aperure

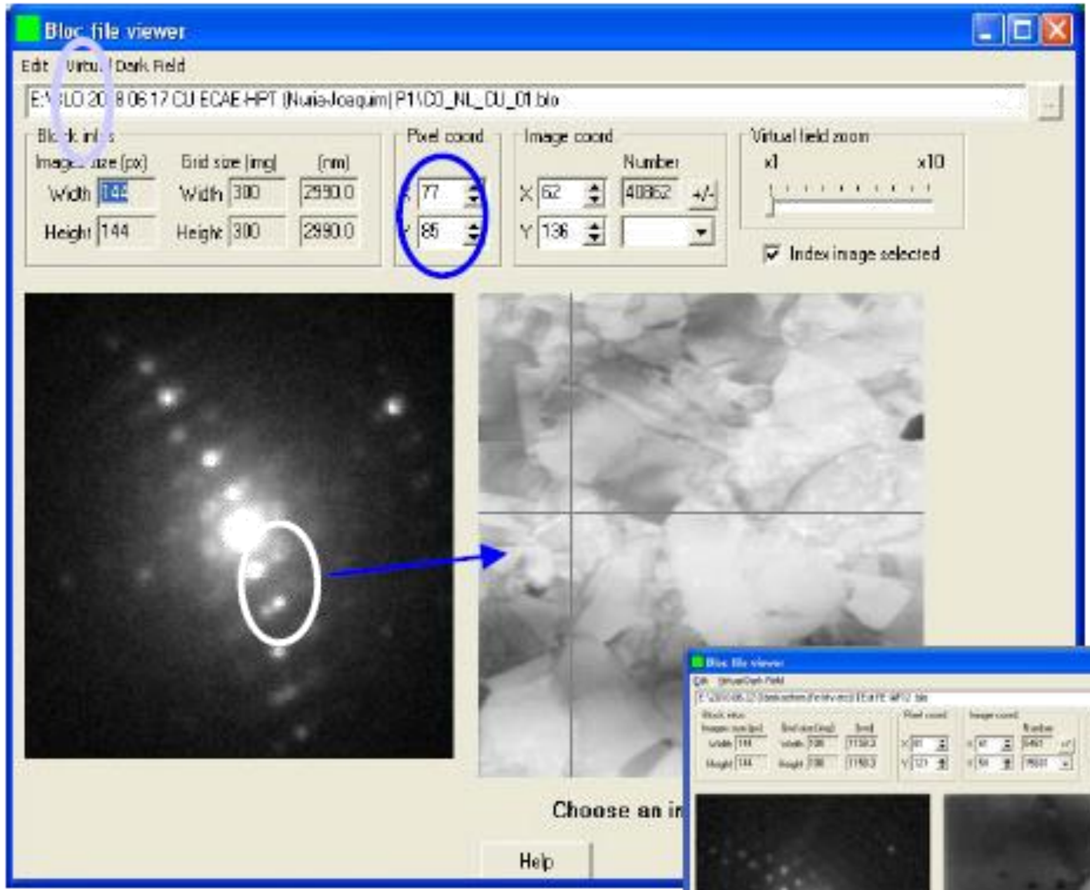

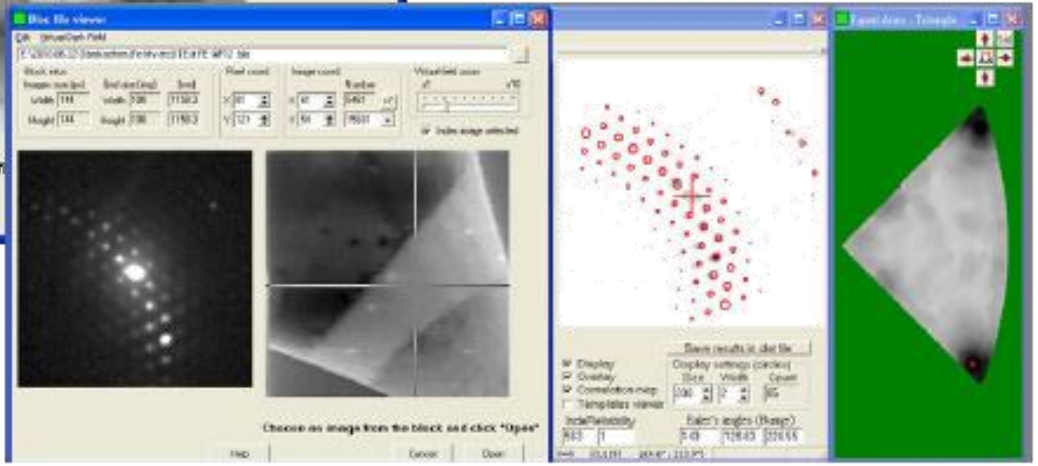

Virtual dark field image

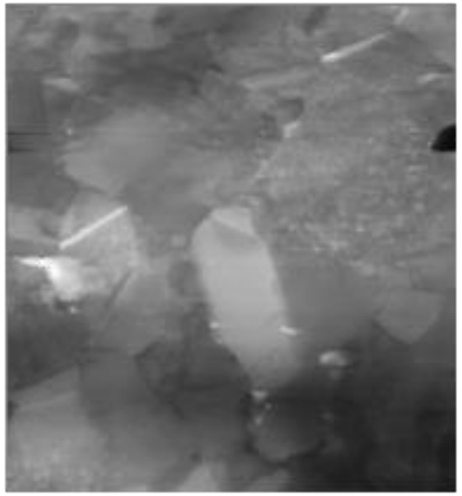

NanoMEGAS
Advanced Tools for electron diffraction

TEM orientation imaging : Phase maps with and without precession

3 existing phases: only possible to distinguish by precession

Orientation map

crystal phase map

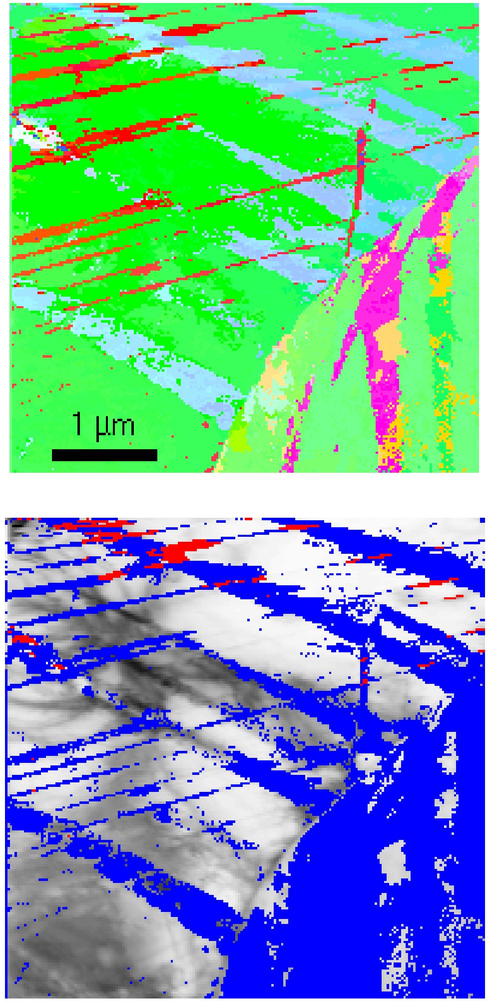

non-precessed

precession 0.4º

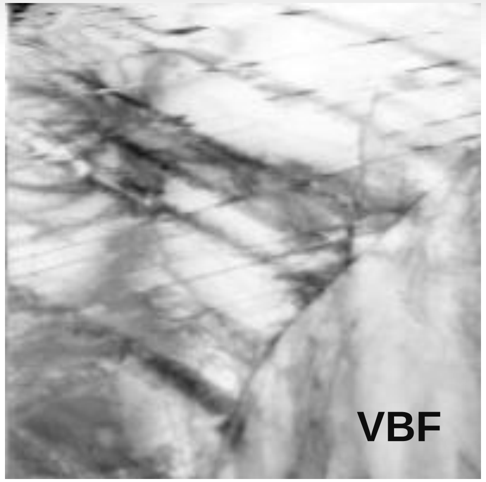

When stacking faults cross themselves, they produce locally a martensite structure (a= 2.87 A)

Austenitic matrix with fcc structure (a=3.58 A)

Stacking faults with hexagonal structure (a=2.57 c= 4.08 A)

In-situ ASTAR STEM characterization In-situ Orientation Imaging ncAu

map 0: 0% strain
initial state

map 7: 4.6% strain
beginning of loading

straining direction

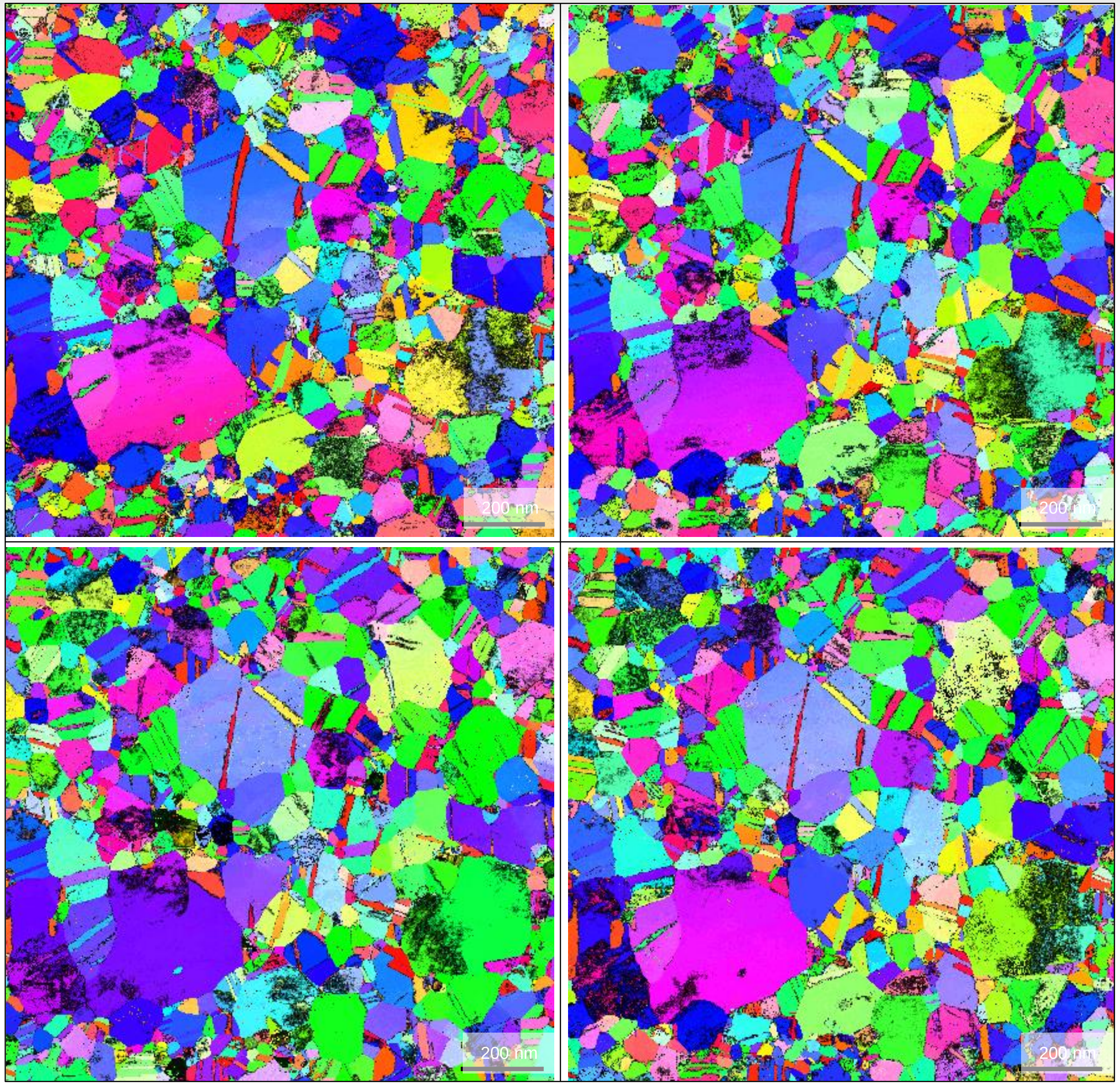

map 9: 6.5% strain
middle of loading

map 11: 9.7% strain
raptured

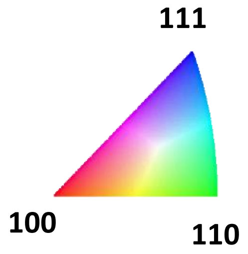

A. Kobler, H. Hahn, C. Kübel, *Ultramicroscopy* **2013**, online

3d data: Traditional approach – tilt series of oriented diffraction patterns

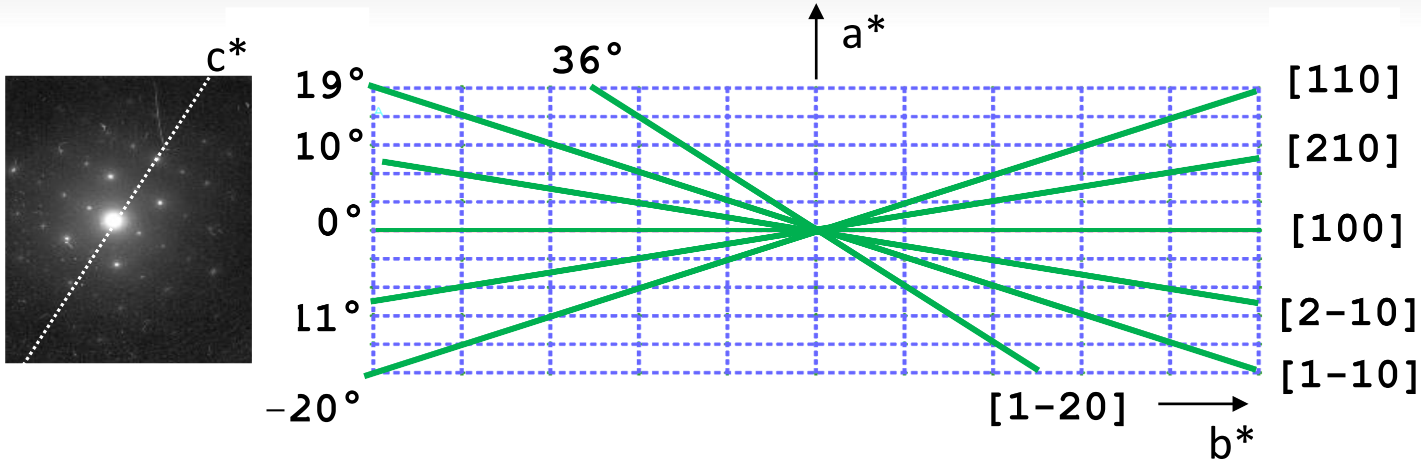

ζ-phase Pigment Red 53:2

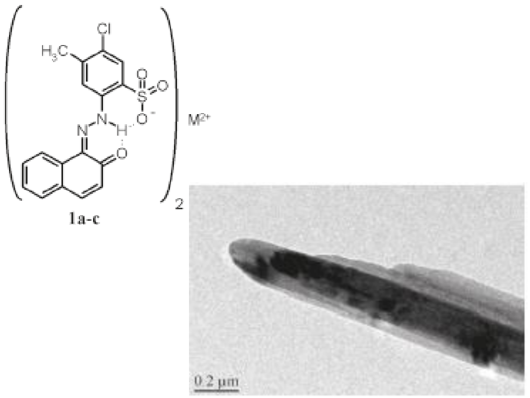

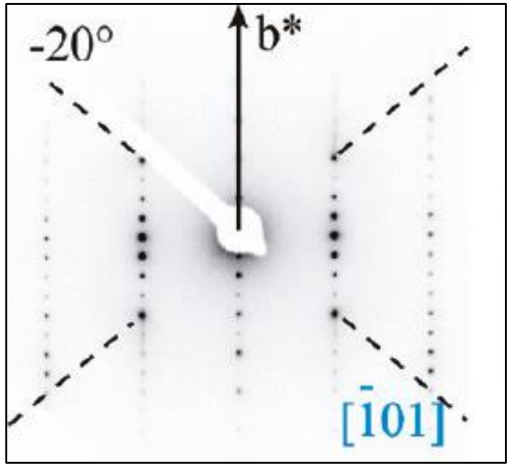

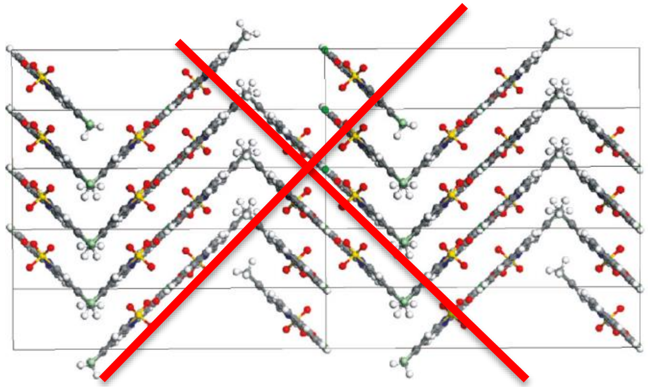

T. Gorelik, U. Kolb, M.U. Schmidt, *Crystal Growth and Design* **47(9)** 3898-3903 (2009).

Ab initio structure solution by direct methods from PED data

single zone

Determination of Nb atom positions
Cell parameters: a = 27.15 Å, b = 21.60 Å, c = 3.95 Å, space group Pbam

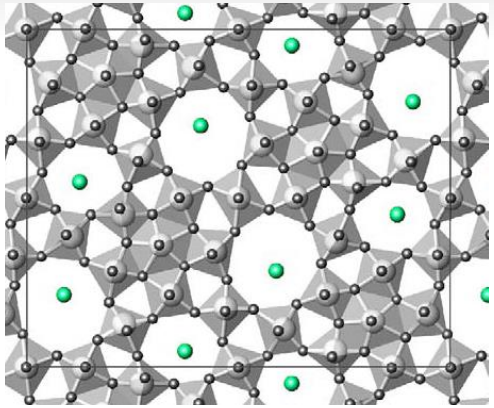

Ab initio determination of the framework structure of the heavy-metal oxide $Cs_xNb_{2.54}W_{2.46}O_{14}$ from 100 kV precession electron diffraction data, Weirich et al., *Ultramicroscopy* **106** 164–175 (2006)

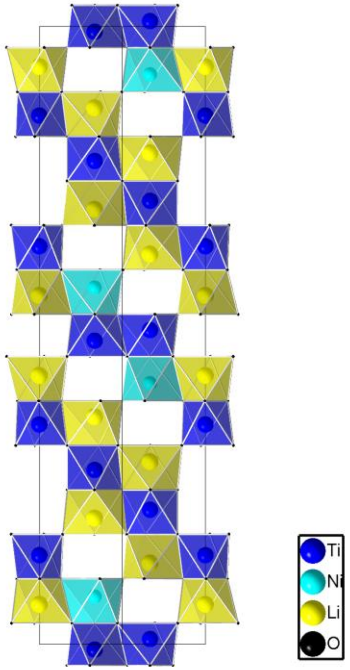

3D data

10 single zone patterns
Cell parameters: a = b = 5.06 Å, c = 32.54 Å, space group P-3c1
refined on Synchrotron XRPD data

Structure solution of the new titanate $Li_4Ti_8Ni_3O_{21}$ using precession electron diffraction. M. Gemmi, H. Klein, A. Rageau, P. Strobelb, F. Le Cras, *Acta Crystallogr B* **66**, 60 (2010).

Crystal Structure of a Lightweight Borohydride from Submicrometer Crystallites by Precession Electron Diffraction. J. Hadermann, A. Abakumov, S. Van Rompaey, T. Perkisas, Y. Filinchuk, G. Van Tendeloo, *Chem Mater* **24**, 3401 (2012).

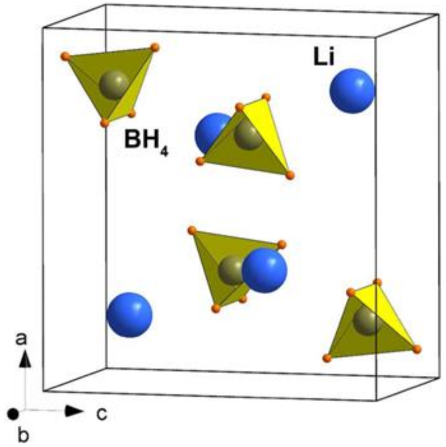

$$I(g) = \int |F(g)\sin(\pi t s_z)/(\pi s_z)|^2 ds_z$$

s_z taken appropriately over the Precession Circuit
t is crystal thickness (column approximation)
ϕ is total precession angle

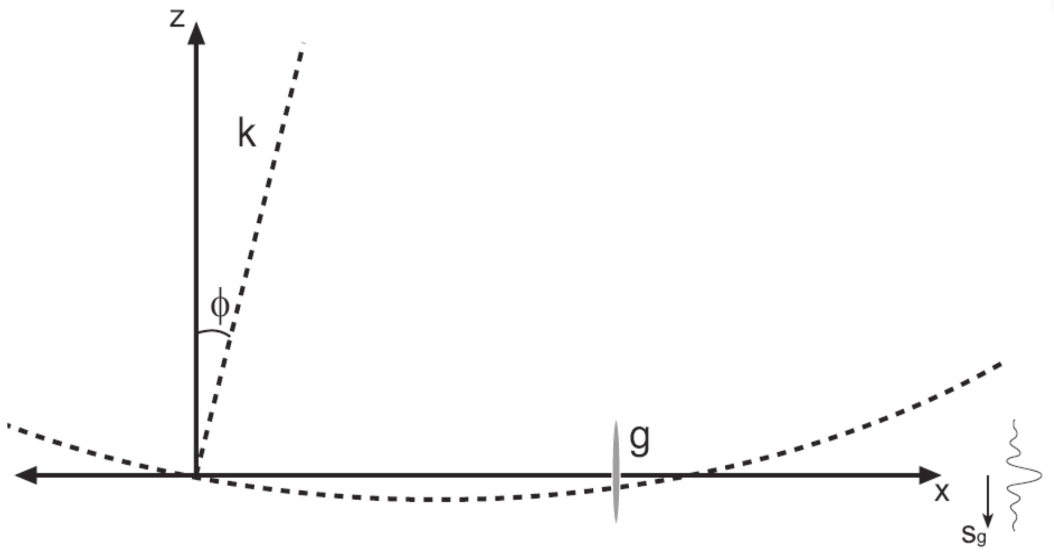

Lorentz Correction: $I(g) = |F(g)|^2 L(g,t,\phi)$

$$L(g,t,\phi) = g\sqrt{1-\left(\frac{g}{2R_0}\right)^2}$$

K. Gjønnes, Ultramicroscopy, 1997.

Blackman 2 Beam approximation: $$I_{Blackman}(t) = \int_0^{A_g} J_0(2x)dx;\ A_g(k) \propto tF(k)$$

Multislice Calculation: $$s_z^{eff} = (s_z^2 + 1/\xi_g^2)^{1/2} \qquad \xi_g = \frac{\pi V_c \cos\theta_B}{\lambda F_g}$$

Completeness of diffraction data

Tilt series: Prominent zones from oriented single crystal selected

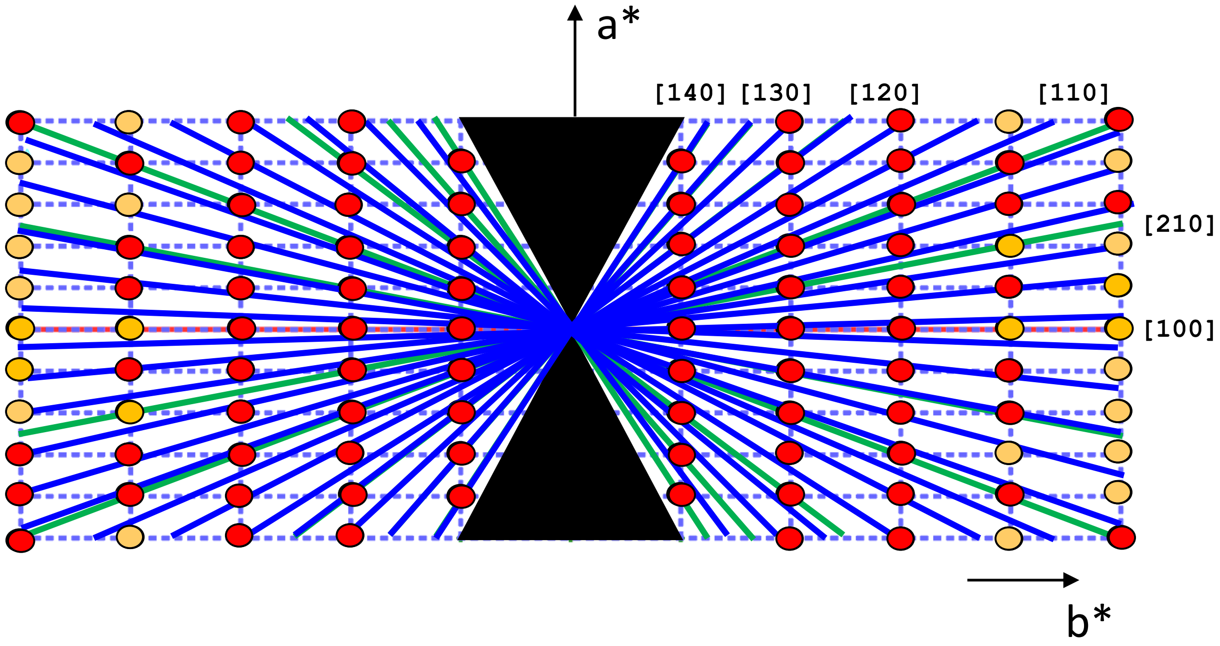

Unaccessible area 20°-60°

Quick and easy (off-zone diffraction: no crystal orientation needed)

Enhanced number of intensities

ADT data collection sequence – with and without precession

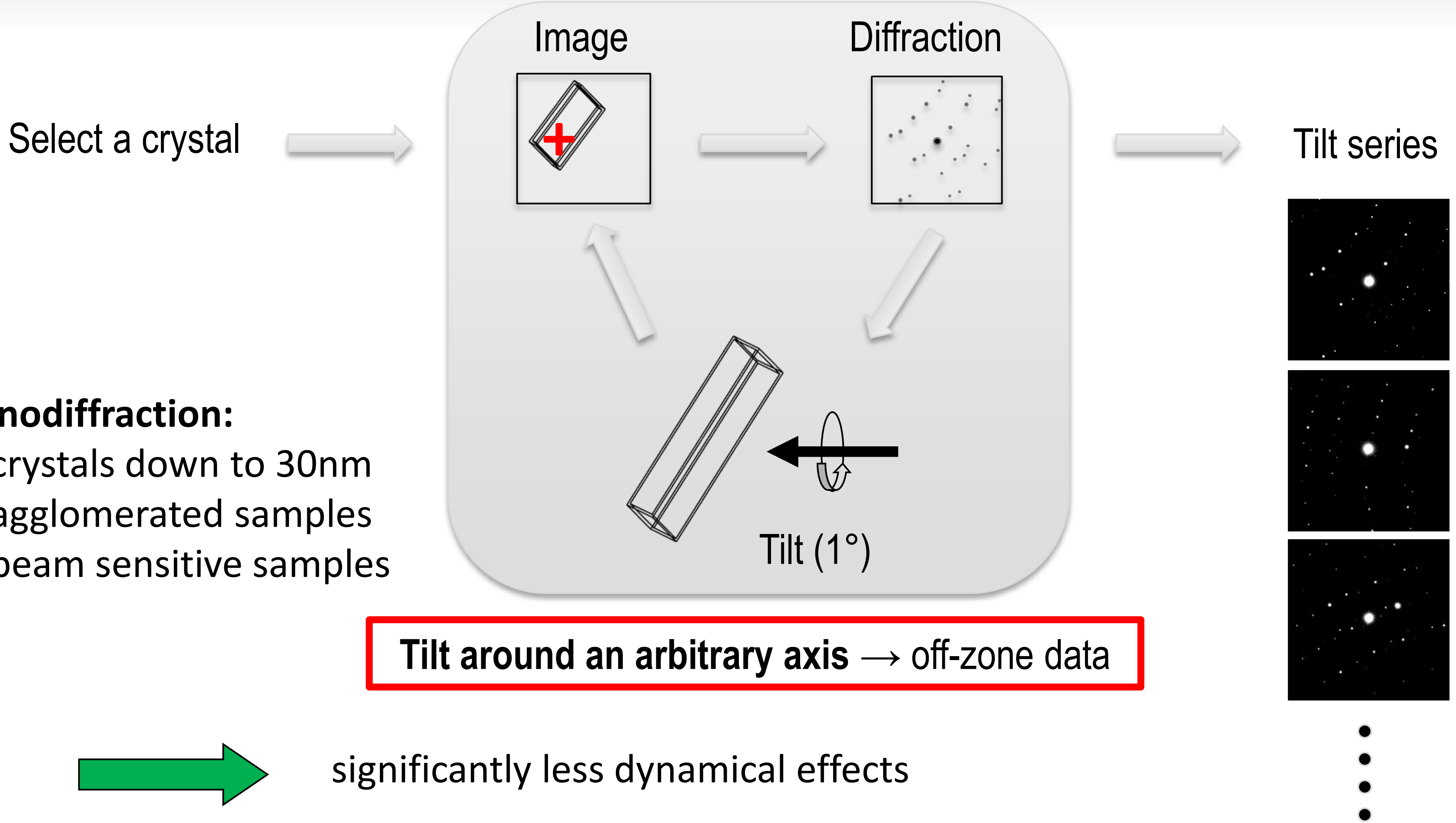

Nanodiffraction:
→crystals down to 30nm
→agglomerated samples
→beam sensitive samples

Tilt around an arbitrary axis → off-zone data

→ significantly less dynamical effects

→ further enhancement of the number of independent intensities

Completeness of the reciprocal space is crucial for structure determination

Taking care of camera length calibration

The additional focussing introduces rotation and contraction/expansion of the pattern → change of the camera length

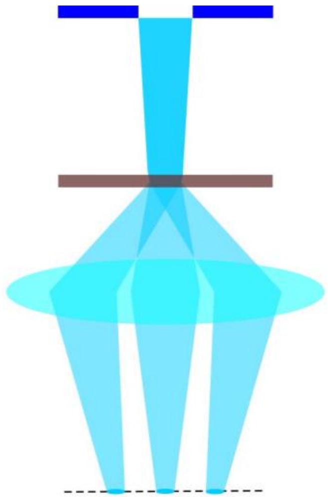

Nanodiffraction

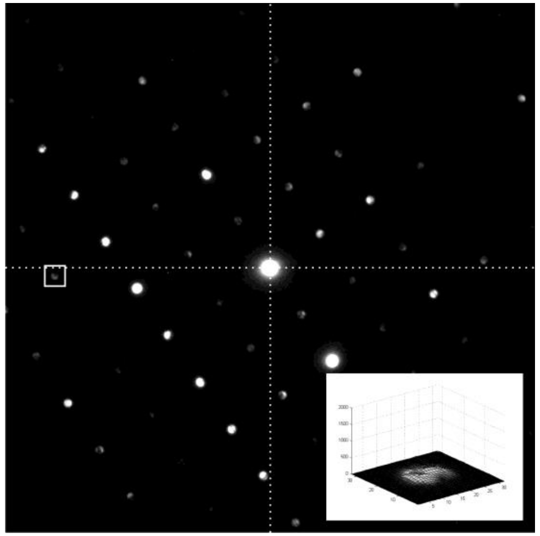

Nanodiffraction pattern

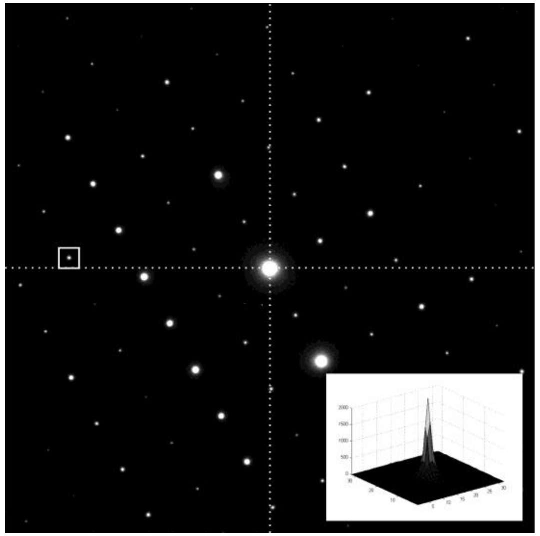

focus into spotty pattern using the diffraction lens

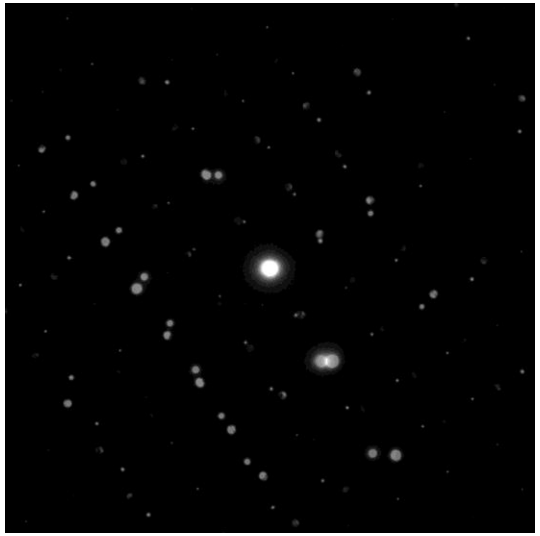

overlay

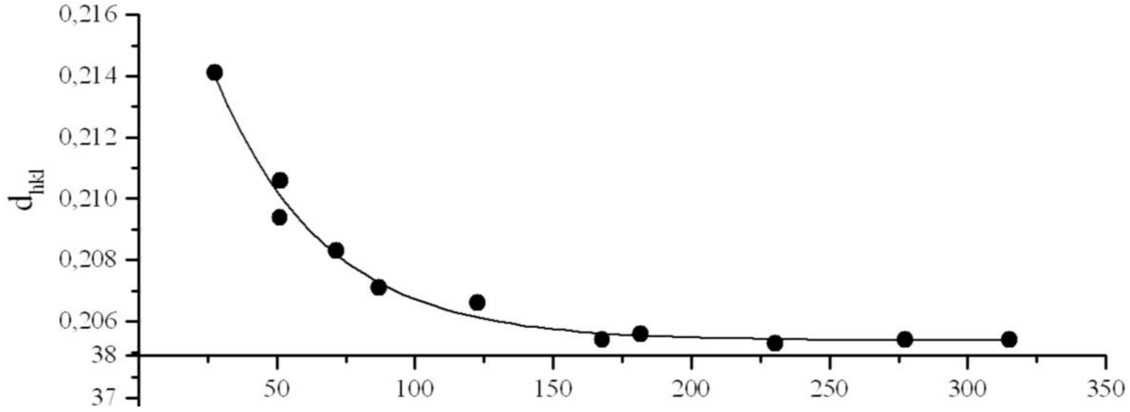

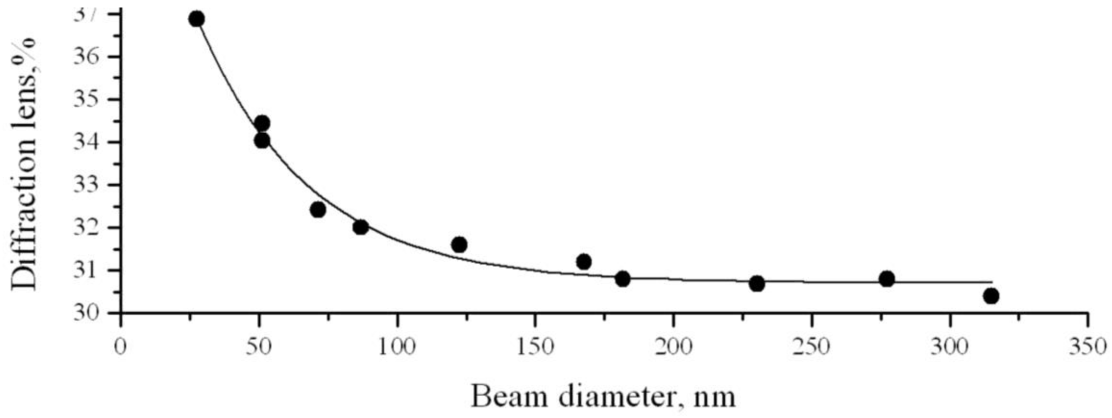

Tomography of the reciprocal space - ADT

Real Space Tomography

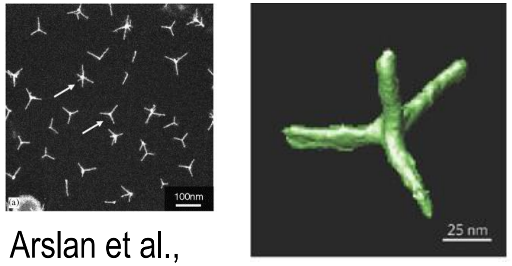

Arslan et al.,
Ultramicroscopy **106**,
994–1000 (2006)

Reciprocal Space Tomography

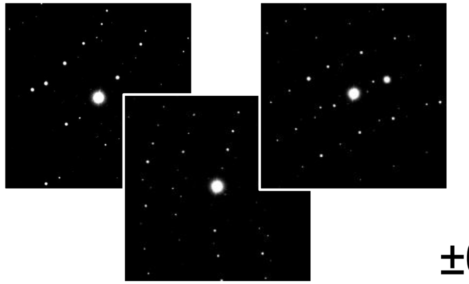

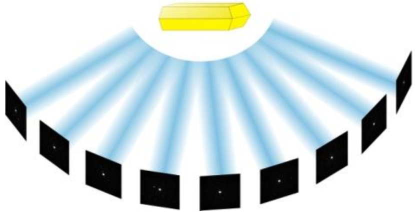

±60° = 121 diffraction patterns
Approx. 2h data collection time

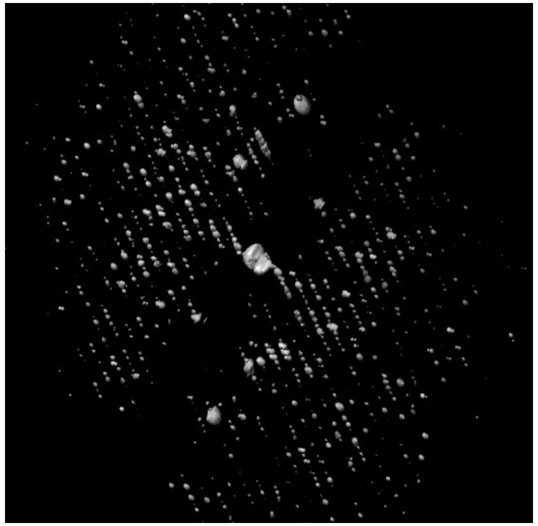

3D reconstructed reciprocal space

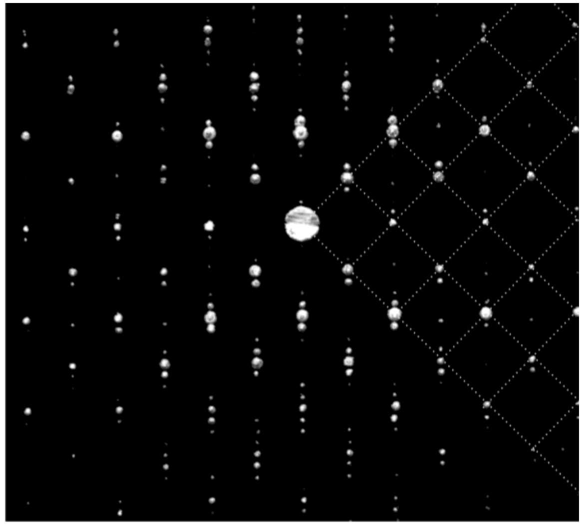

$Bi_{12}O_{17}Cl_2$: superstructure

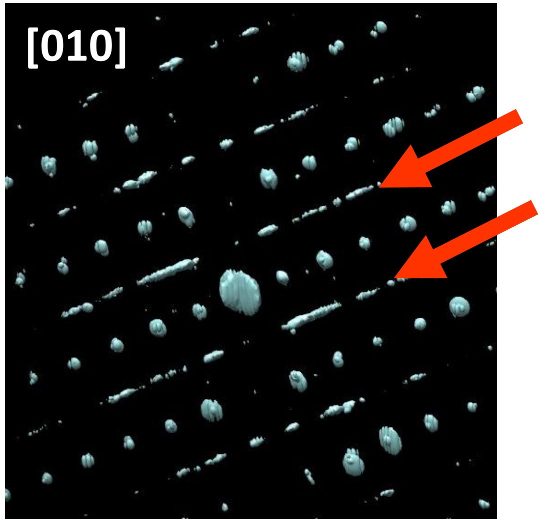

$Li_2O/Al_2O_3/WO_3$: disordered

Steps necessary to reconstruct the reciprocal space

Diffraction data acquisition

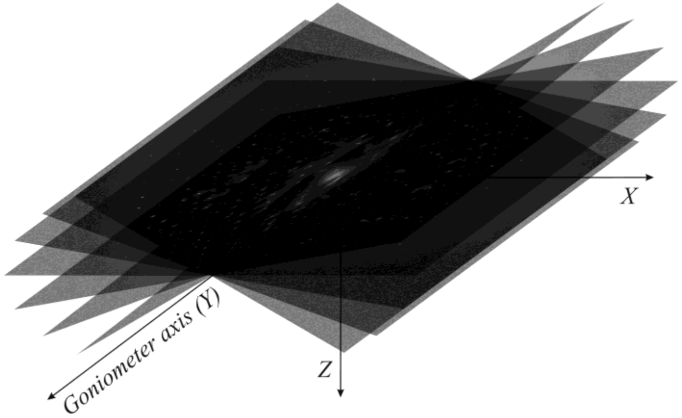

Diffraction data stack

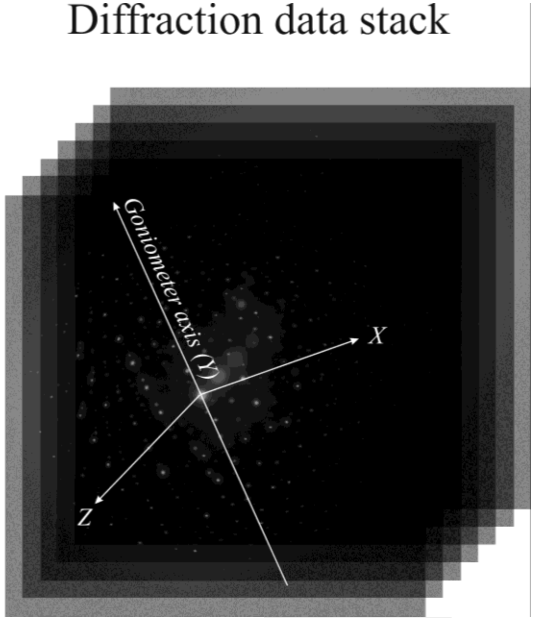

Crystal tracking by beam shift → diffraction shift
(SAED small, NED more sensitive)

Finding the correct tilt axis

Find tilt axis azimuthal angle

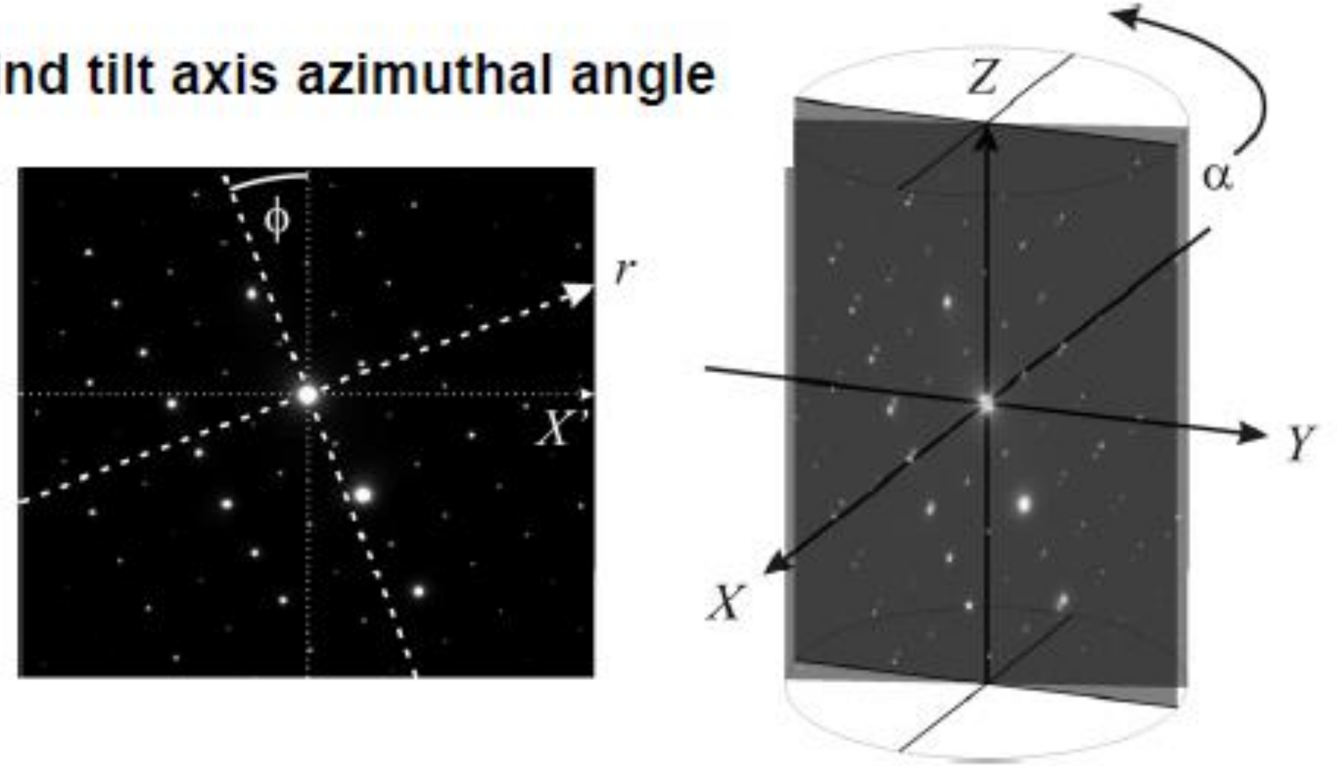

Importance of correct tilt axis

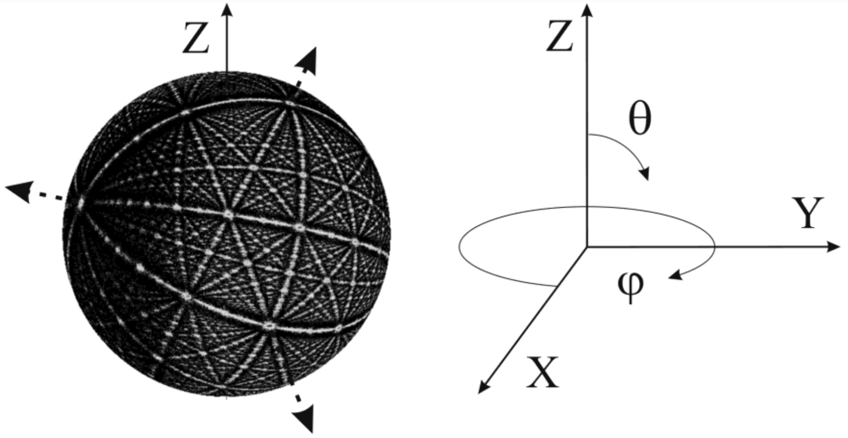

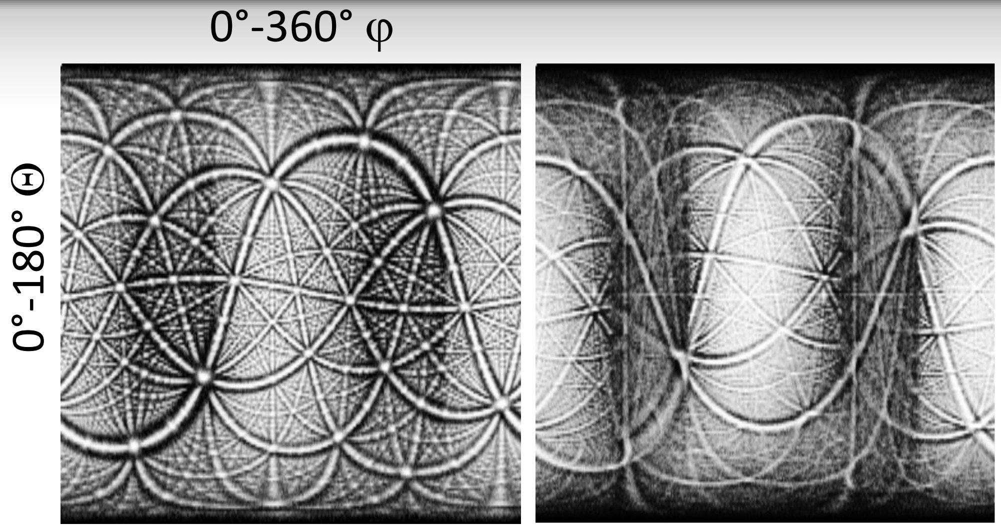

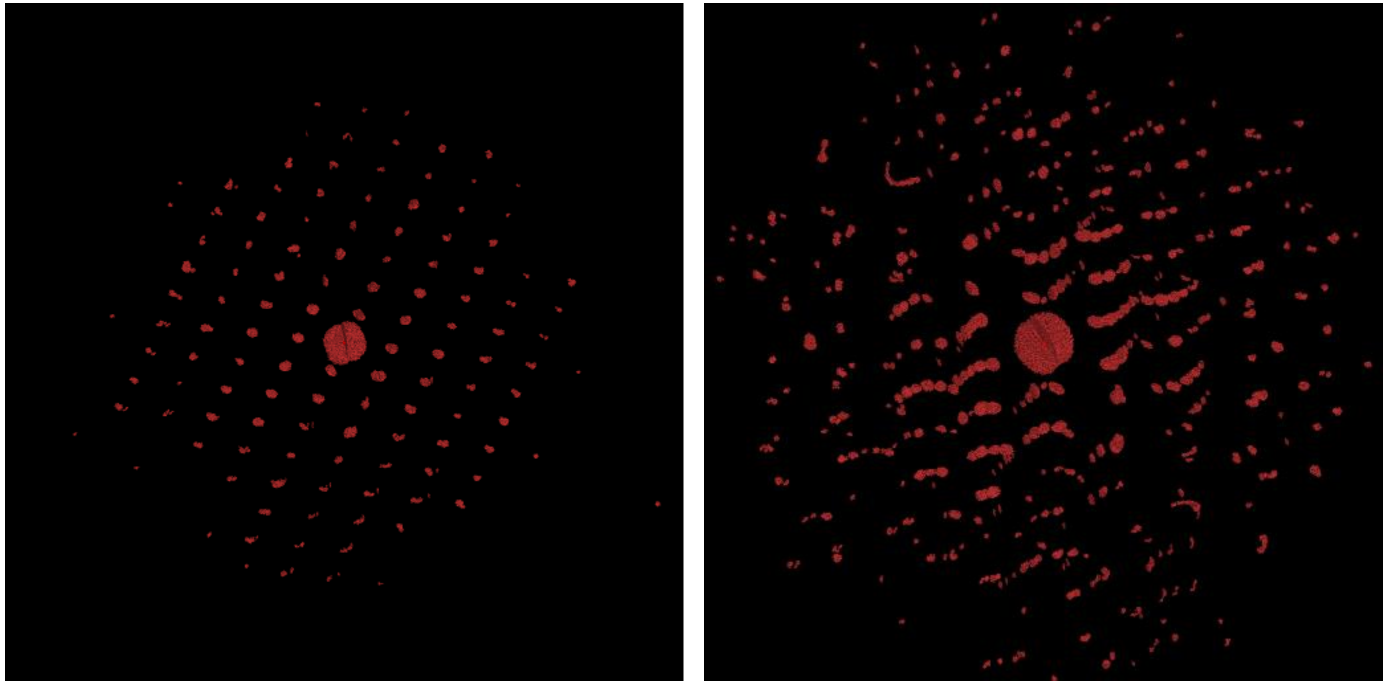

Tilt axis 10° off

ADT – cell parameter determination using difference vector space

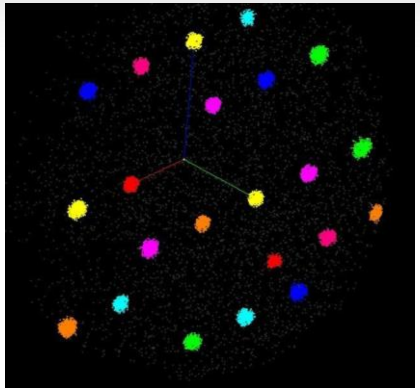

Cell parameter determination

by Clusteranalysis

Error of approx. 2% and triclinic cells directly accessible

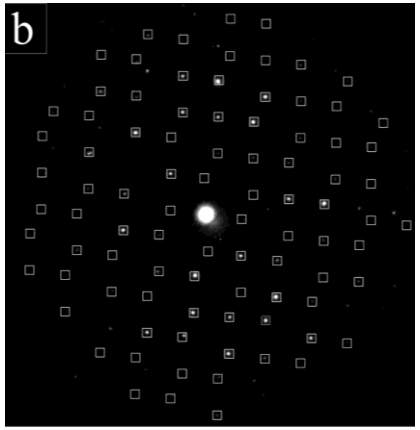

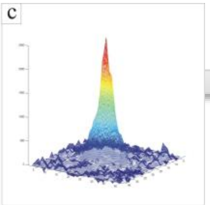

Peakintegration after fine background substraction

Dataset h,k,l Int for „ab-initio“ structure solution using X-ray programs

No further correction is performed on the extracted electron diffraction data

U. Kolb, T. Gorelik and M.T. Otten, *Ultramicroscopy*, **108**, 763-772 (2008).

Indexing the facets: Silikalit-I and 50nm Au nanorod

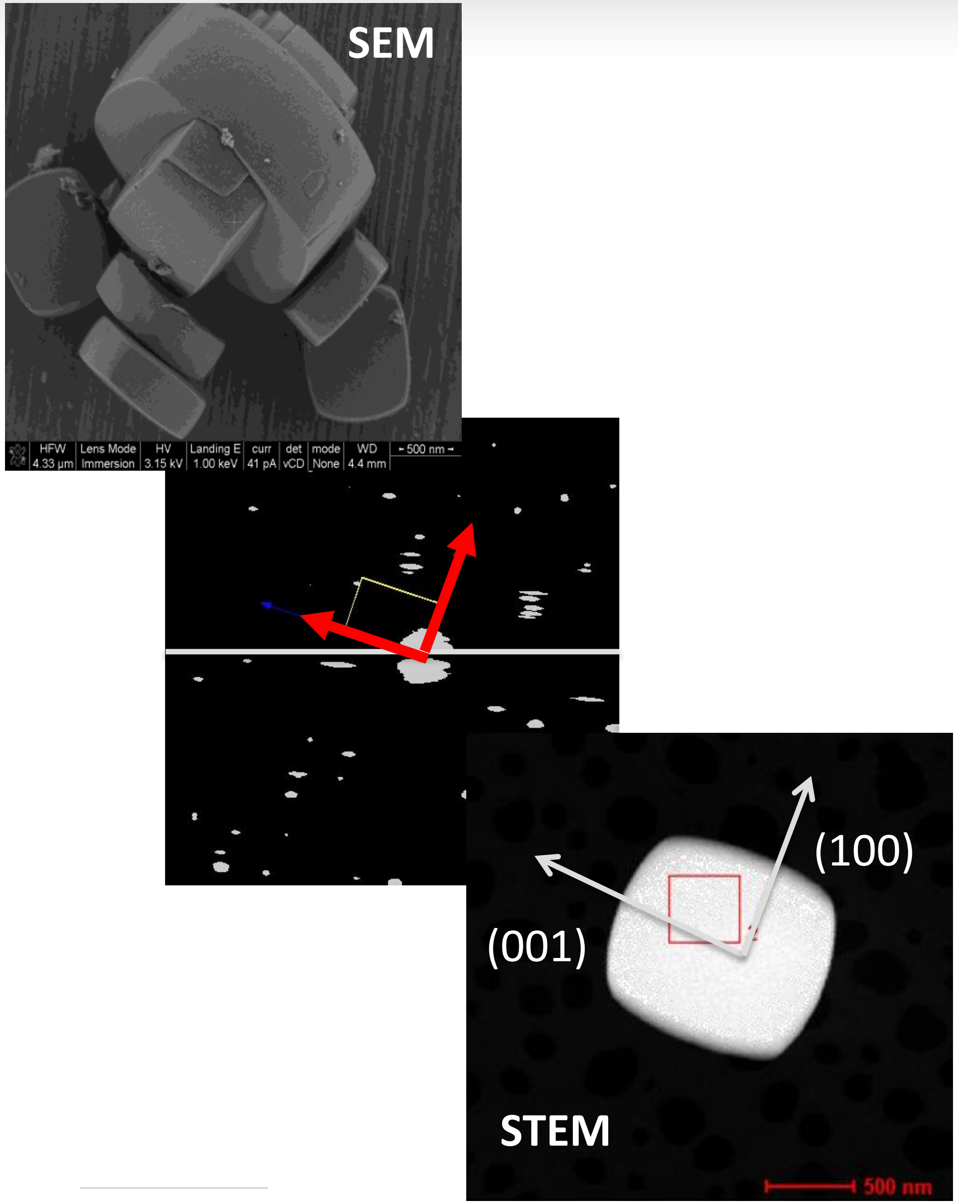

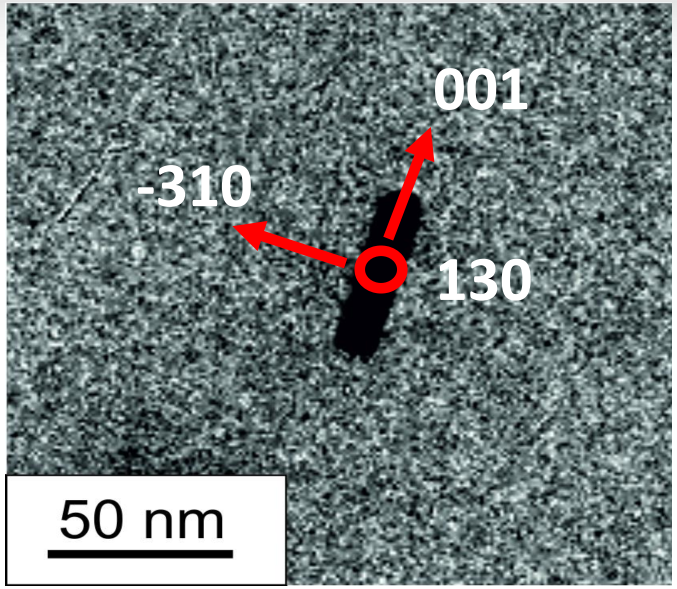

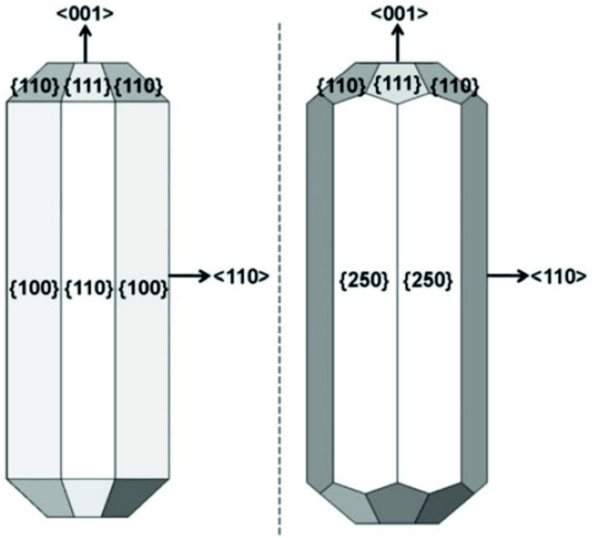

Wang et al. 1999

Carbó-Argibay et al. 2010

Katz-Boon H et al. 2011

ADT - Space group determination and intensity extraction

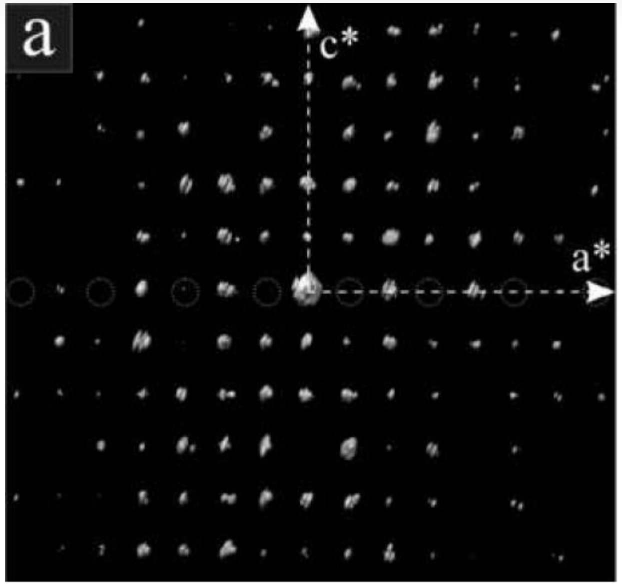

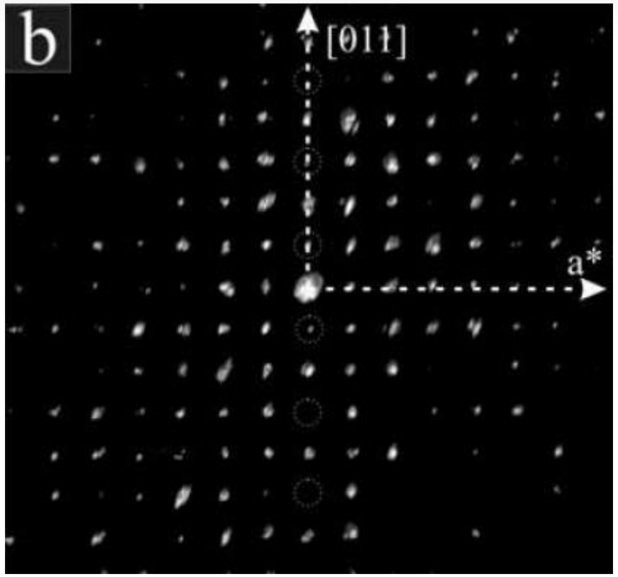

Barite ($BaSO_4$):

a = 8.884 Å, b = 5.458 Å, c = 7.153 Å, V= 346 $Å^3$
Space group **Pnma** found directly by SIR08, only minor extinction violations

355 of 375 possible reflections at 0.7 Å resolution
95% coverage of reciprocal space

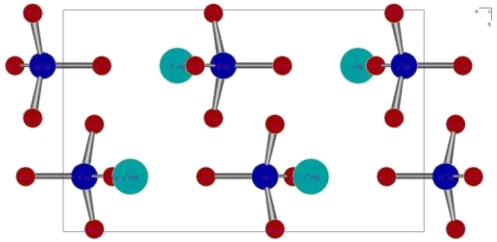

Zonal data: Ba, S
ADT: Ba, S, 2O
ADT+PED: Ba, S, 3O
Max. dev: 0.06 Å

Structure solution of known structures

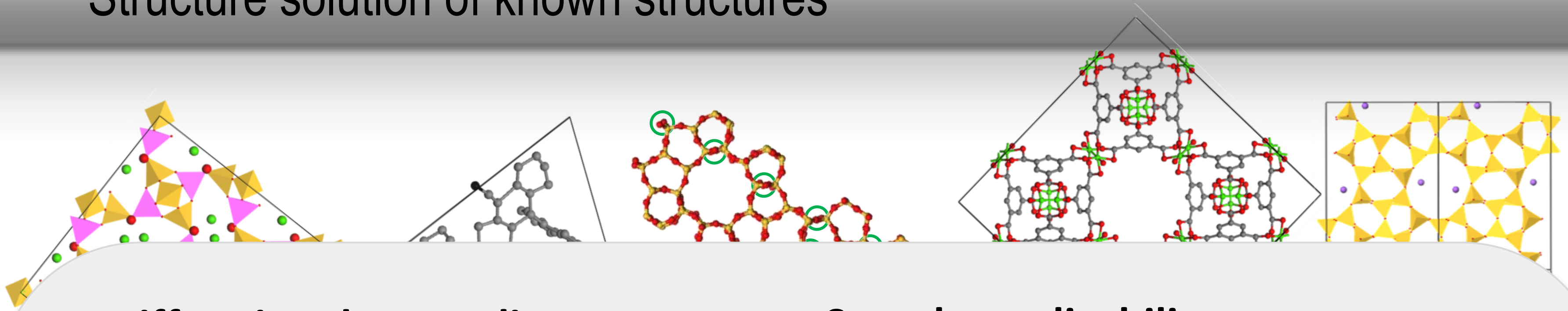

Diffraction data quality:

Completeness of diffraction space
~70% triclinic
~90% monoclinic

Resolution: ~0.08 nm organics
~0.06 nm inorganics

Average deviation of atomic positions (comparison ADT - X-ray): ≤ 0.01 nm

Good detectability of light atoms

Sample applicability:

Smallest crystal used:
~300 nm organics
~ 30 nm inorganics

Largest analysed volume: 33000 Å^3

Largest number of independent atoms: 90

Agglomerated and embedded samples
Polyphasic materials
Highly beam sensitive material

$Na_4Ti_6O_{14}$	Cm	436	24	6	0,8	58%
$Na_2W_2O_7$	Cmce	454	9	18	0,9	91%

Principle of tomography

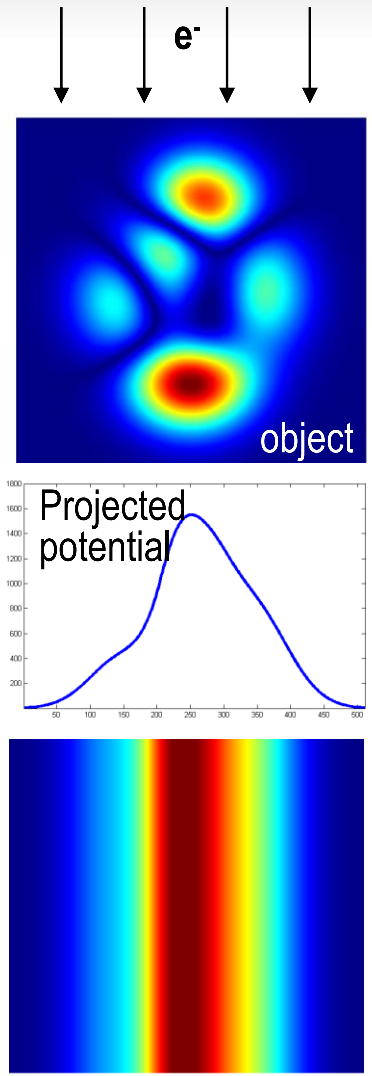

Reconstructed image

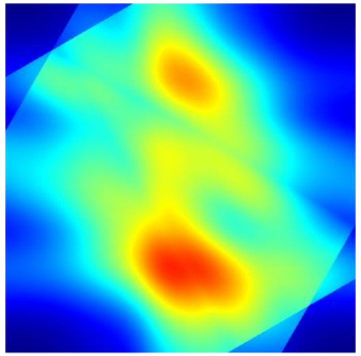

Tomographic
reconstruction

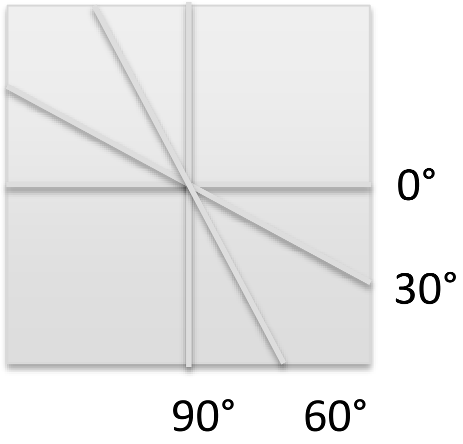

Real space

Image plane

projection of potential

Reciprocal space

Backfocal plane

FT of potential

Missing cone problem: ZSM-5 (twinned crystals)

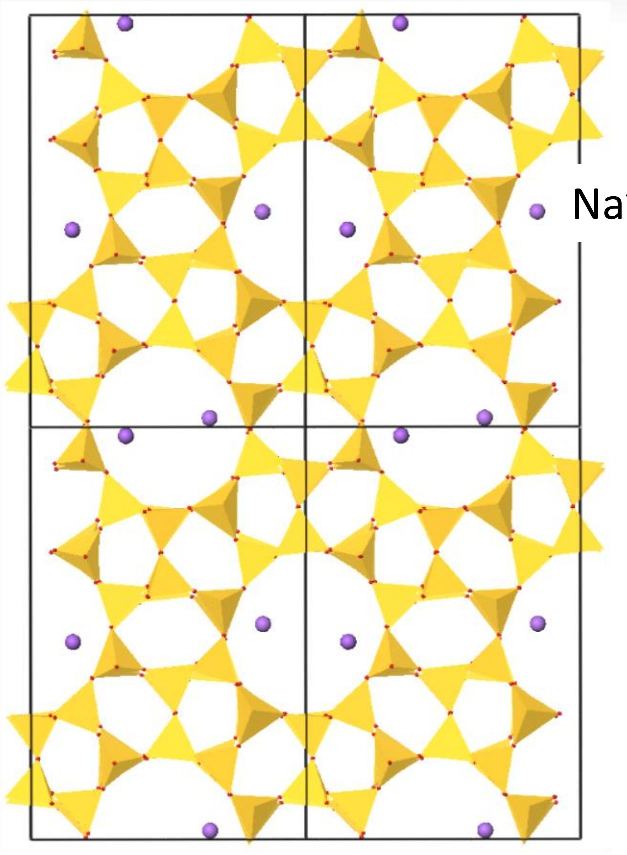

View down b-axis

Pnma: a = 20.1 Å, b = 19.9 Å, c = 13.4 Å, V= 5360 $Å^3$
2288 indep. reflections, completeness 79% mainly reflections in direction a* are missing

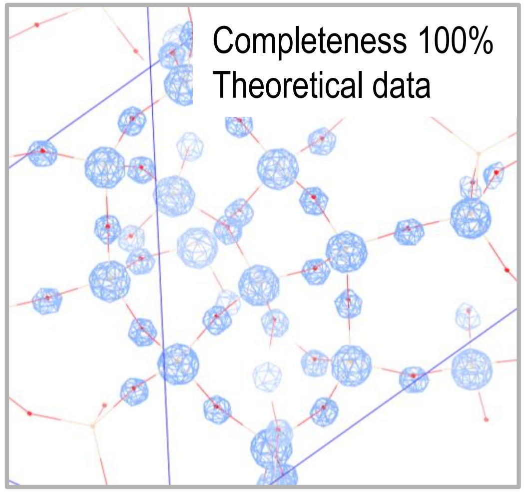

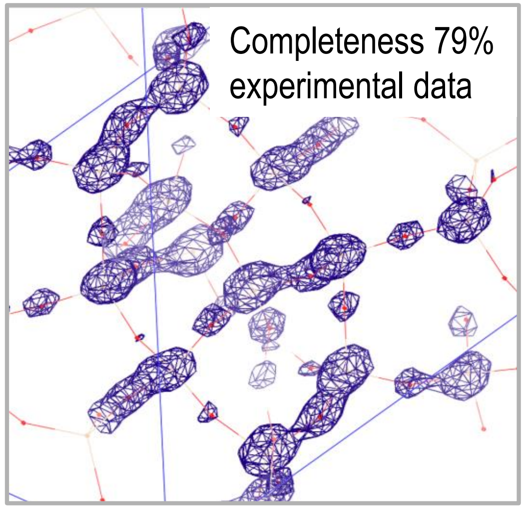

12 T sites; 10-member rings
Si/O determined „ab initio"; Na by fourier map; EDX confirms small amount of Na

Detectability of atoms

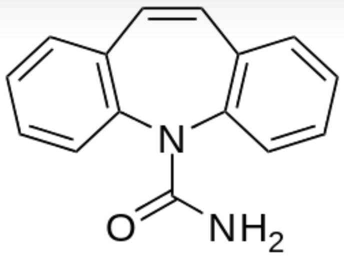

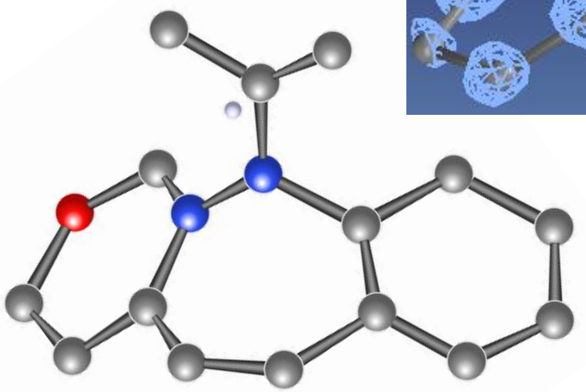

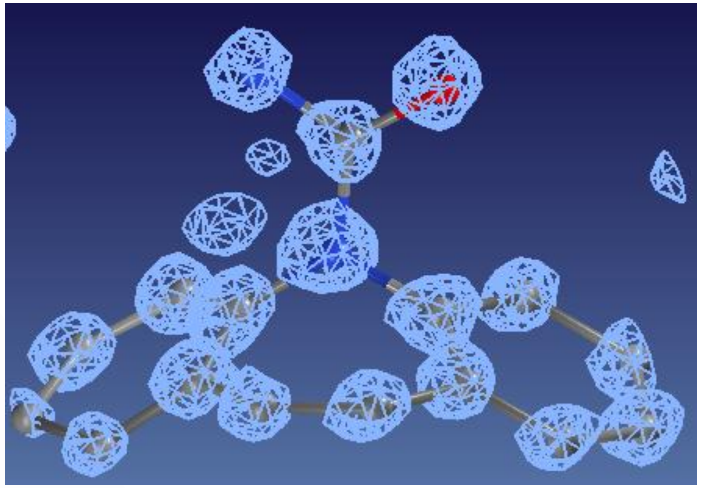

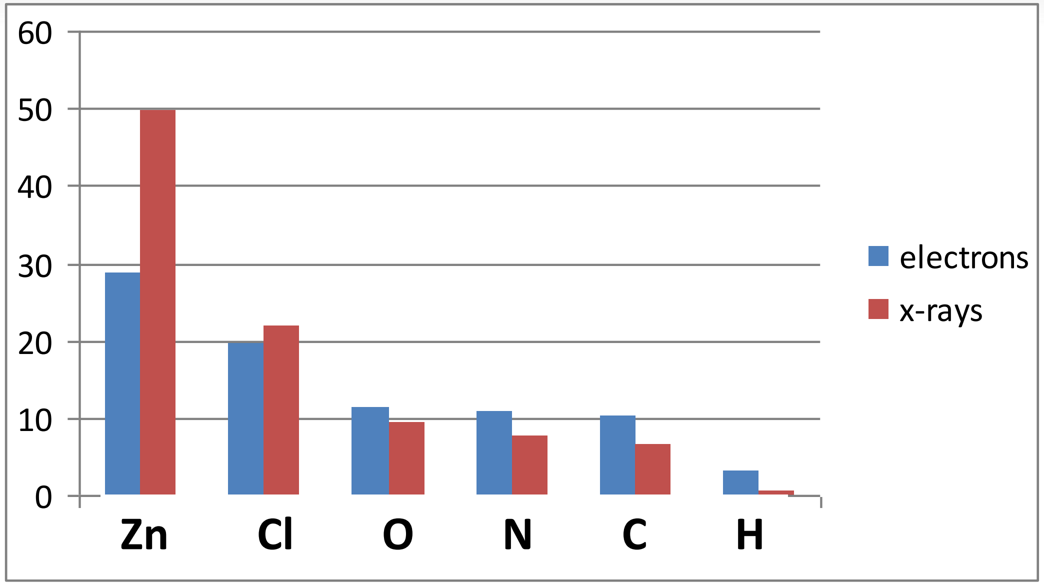

Carbamazepine Polymorph III: Solution „direkt methods“ from SIR14

SIR: M. C. Burla, R. Caliandro, M. Camalli, B. Carrozzini, G. L. Cascarano, C. Giacovazzo, M. Mallamo, A. Mazzone, G. Polidori and R. Spagna, J. Appl. Crystallogr., 2012, 45, 357–361.

Electron radiation:
- atoms are less distinguishable
- light atoms are better visible next to heavy atoms

→ Elemental analysis (EDX) can deliver composition information

Si/Al: distinguishable via bond len
Si/(Ge, Ti, …): chance to find maj

1,5-diaminoanthraquinone (DAAQ) - organic dye

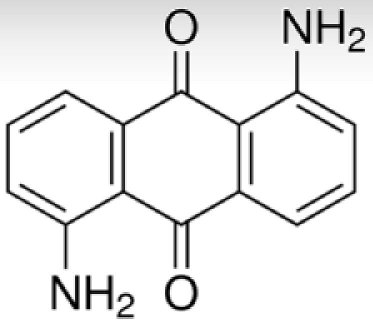

40° ADT data: two atoms missing

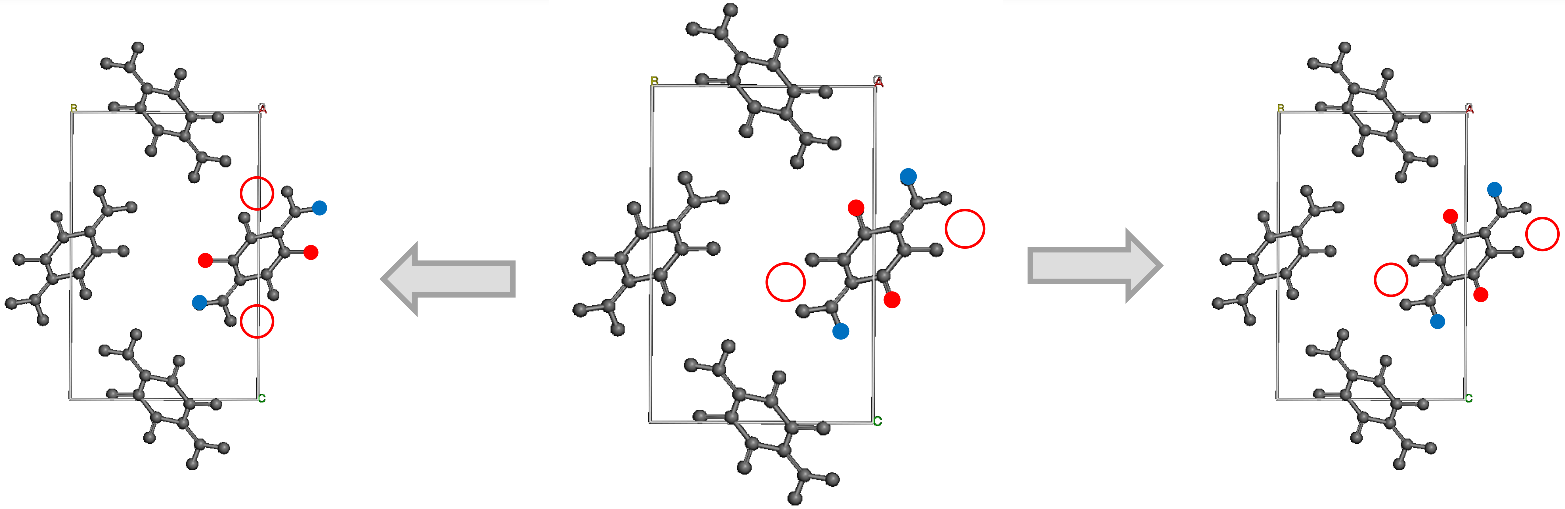

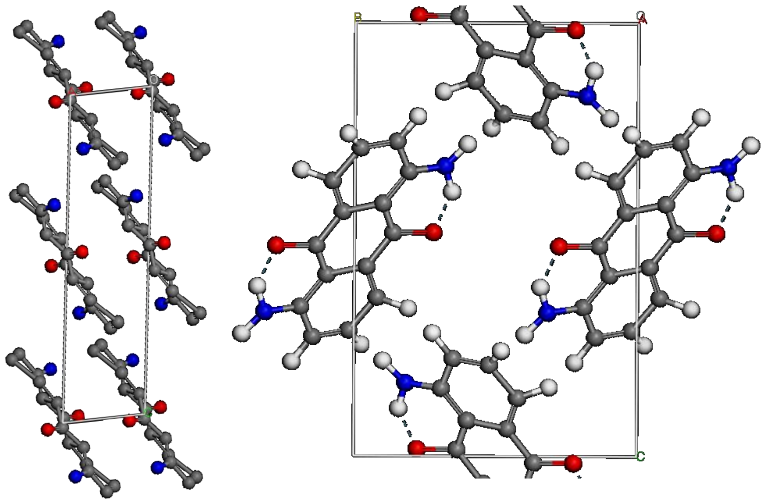

found in Literature: solved from zonal PED data and XRPD

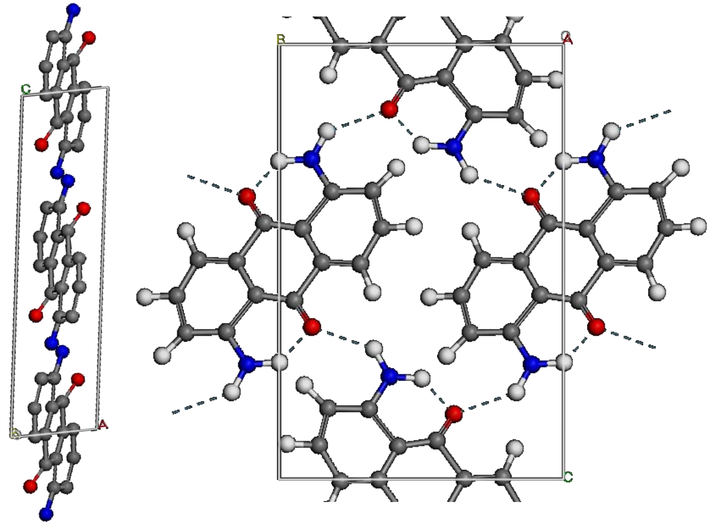

120° ADT data: all atoms detected

Template: Hierarchical Mesomicroporous Zeolite ITQ-43

Si/Ge Zeolite + organic structure-directing agent, framework density 11.4 T-atoms /1000 Å^3

3 sets of 12-ring channels of 6.8 Å× 6.1Å cloverleaf-like channels formed by 28-rings along c axis; pore diameters: 21.9 Å × 19.6 Å

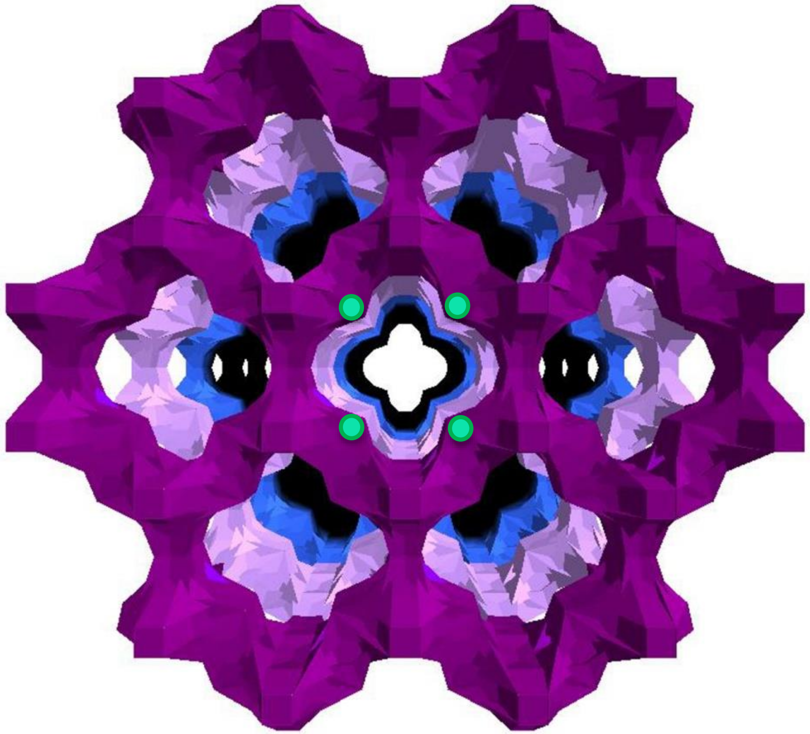

Delta-recycling: Rius, J. (2012)

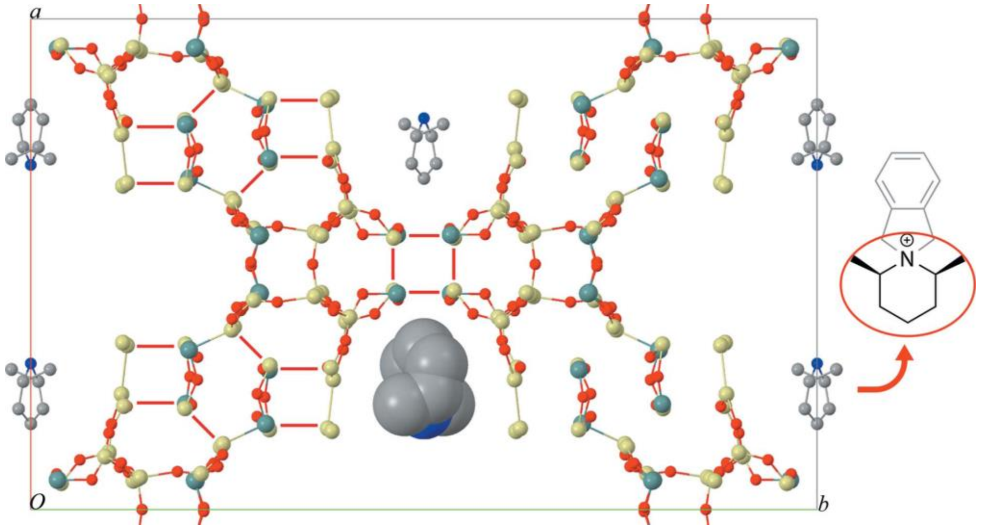

J. Jiang, J. L. Jorda, J. Yu, L. A. Baumes, E. Mugnaioli, M. J. Diaz-Cabanas, U. Kolb, A. Corma, Science, 333(6046),1131-1134 (2011); J. Rius, E. Mugnaioli, O. Vallcorba, U. Kolb, *Acta Cryst.* **A69**, 396–407 (2013)

MOFs – highly beam sensitive material

MFU-4long

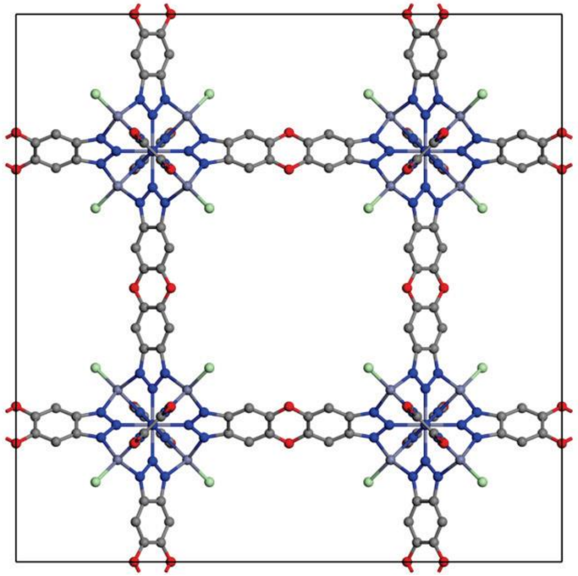

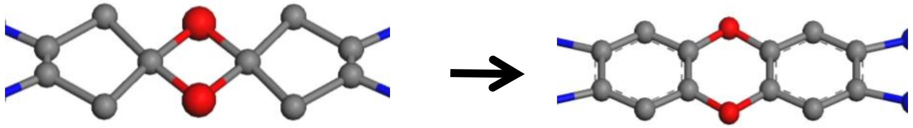

$Fm\text{-}3m$, a=32.0 Å, V = 32,768 Å^3 , resolution 1.3 Å,
R(F)=32%,
max. deviation to XRPD = 0.21 Å

Bi(BTB): twinned crystals

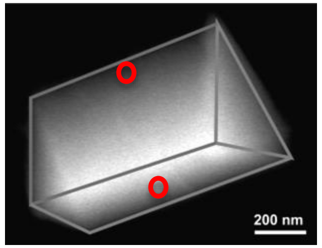

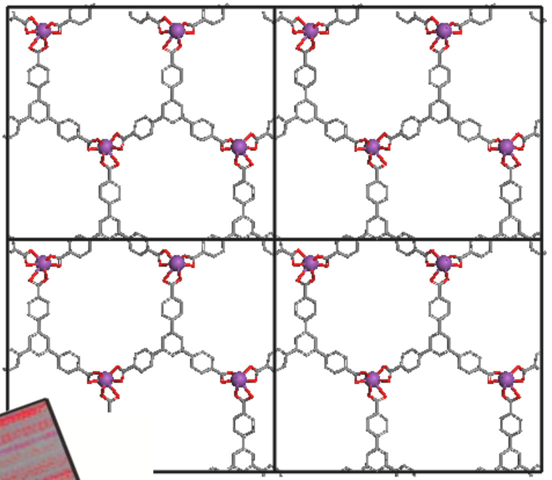

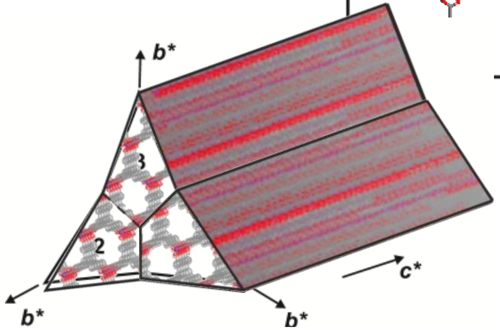

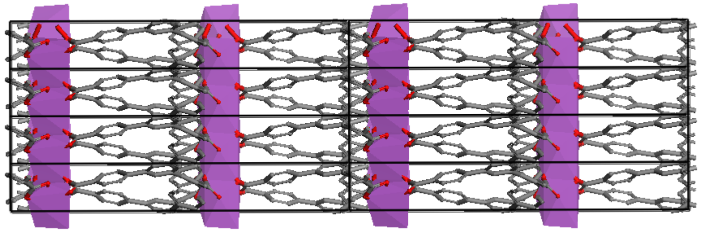

D. Denysenko, M. Grzywa, M. Tonigold, B. Schmitz, I. Krkljus, M. Hirscher, E. Mugnaioli, U. Kolb, J. Hanns and D. Volkmer *ChemistryJ.Eur.* **17(6)**, 1837-1848 (2011); M. Feyand, E. Mugnaioli, F. Vermoortele, B. Bueken, J. Dieterich, T. Reimer, U. Kolb, D. de Vos and N. Stock, *Angewandte Chemie* 124, 10519 –10522 (2012).

High pressure - Hapy (Hydrous Aluminum bearing Pyroxene)

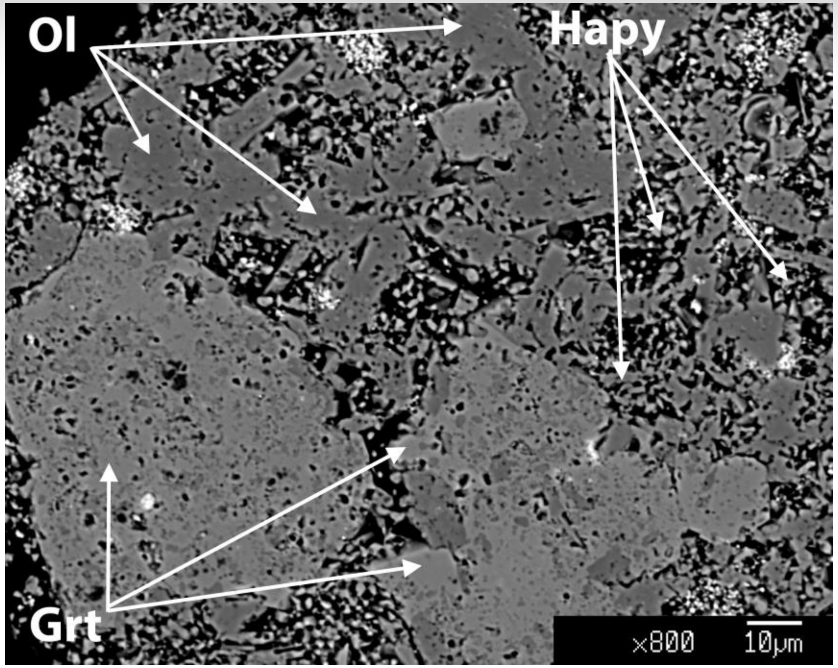

Problem: olivine and garnet + small crystals of a third unknow phase

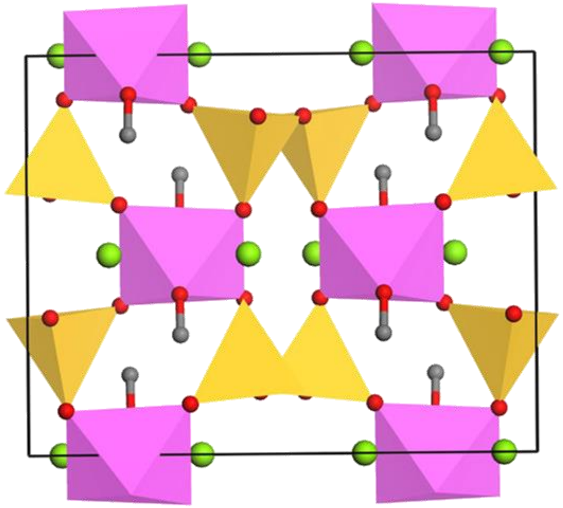

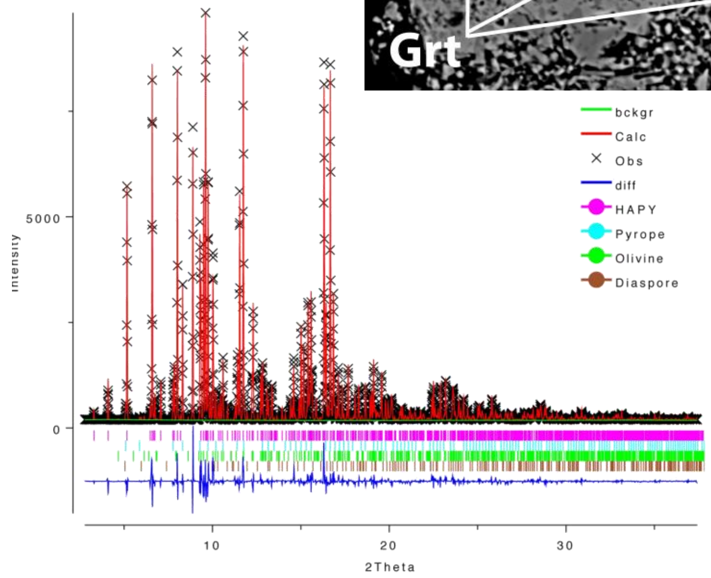

New high-pressure phase synthesized in MgO-Al_2O_3-SiO_2-H_2O system

Not detected by optical microscope and by X-ray powder diffraction.

Re-synthesized after structure solution and refined versa x-ray powder data

A new hydrous Al-bearing pyroxene as a possible water carrier in the subduction zones, M. Gemmi, J. Fischer, M. Merlini, P. Fumagalli, S. Poli, E. Mugnaioli, U. Kolb, *Earth and Planetary Science Letters* **310** 422-428 (2011)

High pressure – boron oxo nitride ($B_6N_4O_3$)

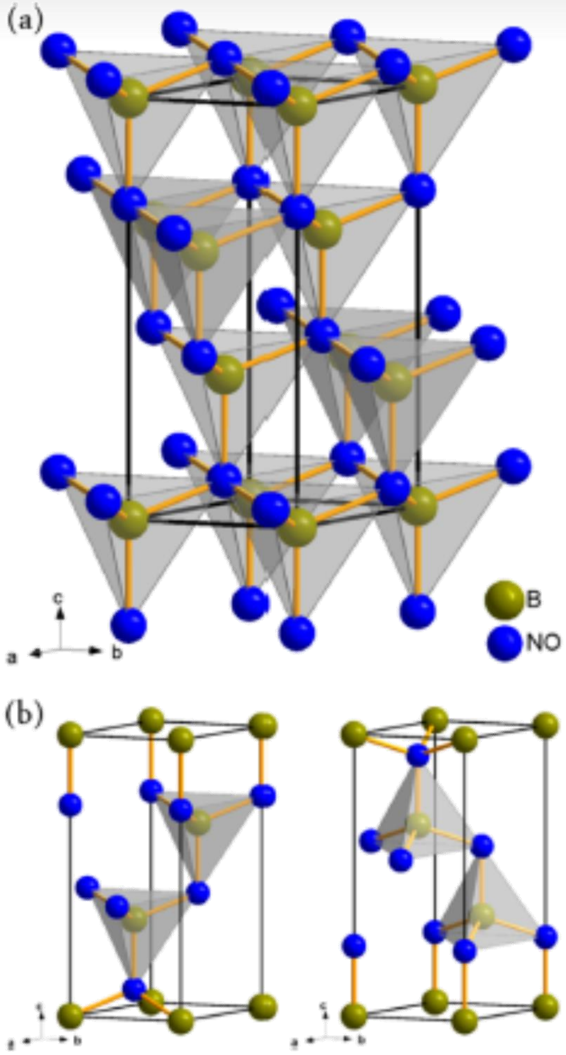

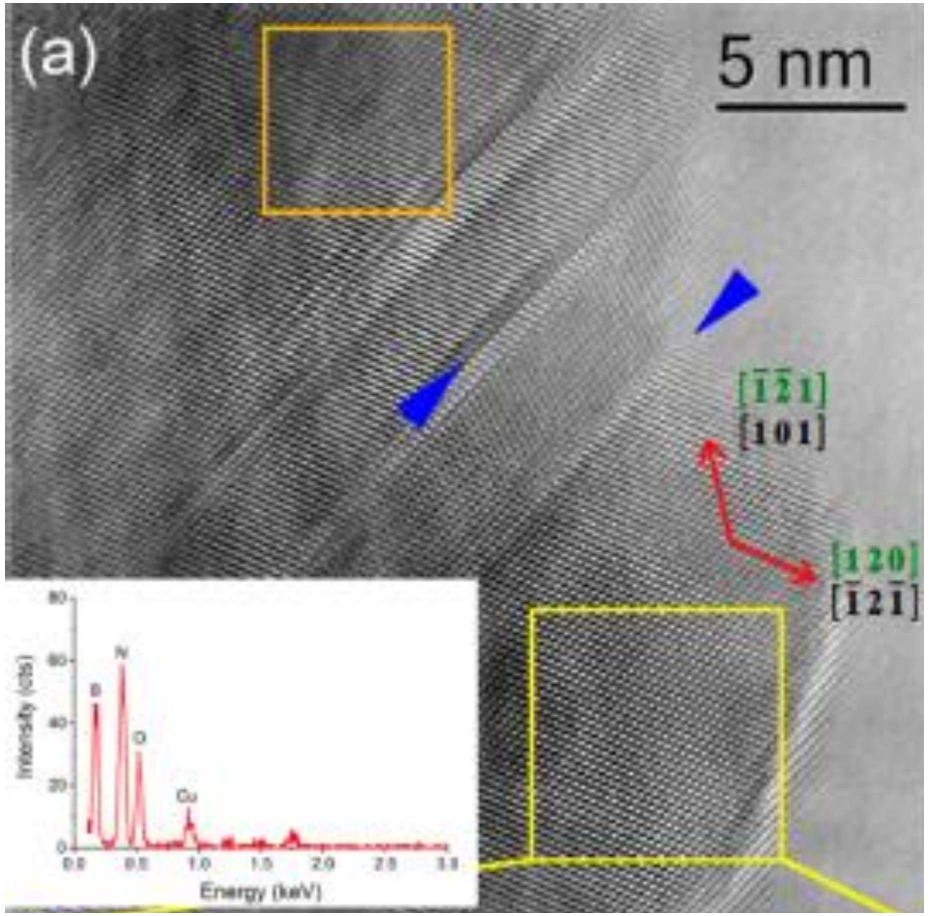

Triangular platelets <50nm (EELS: B:N:O = 6:4:3)

S. Bhat, L. Wiehl, L. Molina-Luna, E. Mugnaioli, S. Lauterbach, S. Sicolo, P. Kroll, M. Duerrschnabel, N. Nishiyama, U. Kolb, K. Albe, H.-J. Kleebe and R. Riedel, Chem. Mater. 2015 (in print)

Charoite - Murun Massif in Yakutiya, Sakha Republic, Siberia, Russia

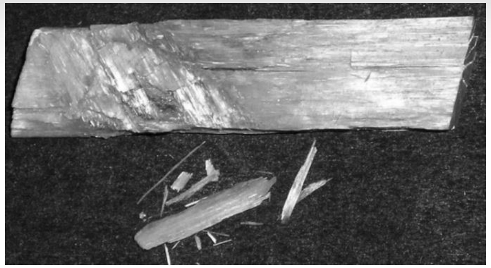

- asbestos-like fibres typically around 200 nm diameter
- two phases: fibre axes almost parallel, a and b differently oriented
- fibres are laterally separated by an amorphous phase

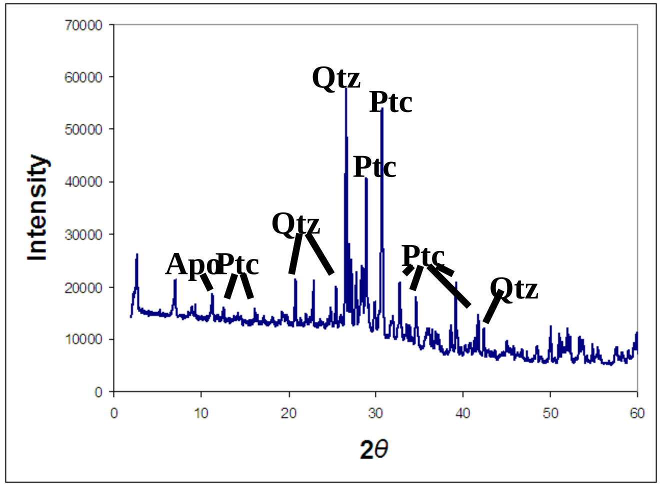

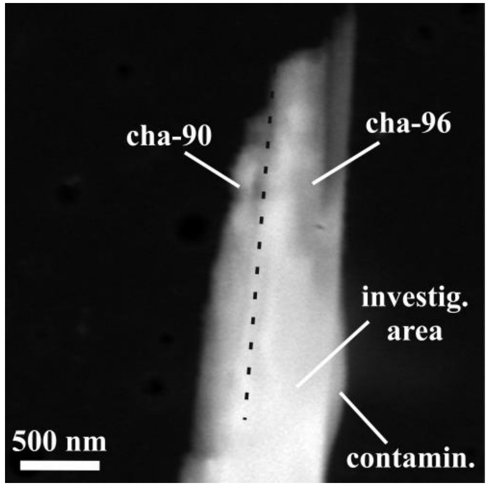

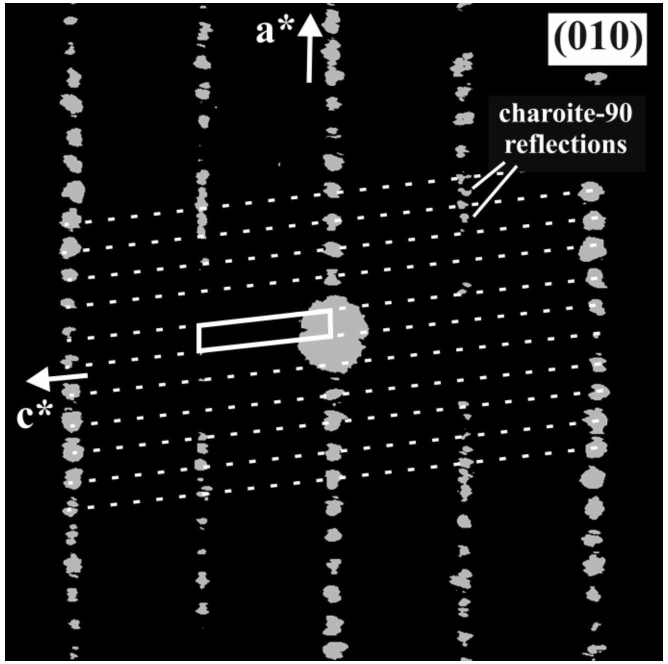

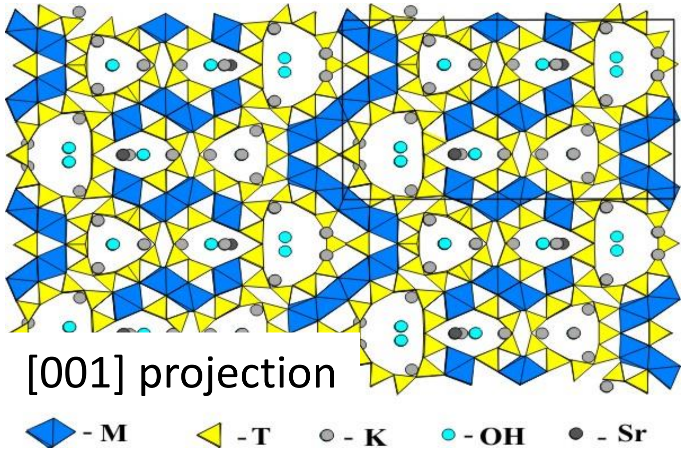

Charoite-90: space group $P2_1/m$
a=31.96 Å, b=19.64 Å, c=7.09 Å, β=90°
Charoite-96: space group $P2_1/m$
a=32.11 Å, b=19.67 Å, c=7.23 Å, β=95,9°

I. Rozhdestvenskaya et al., *Mineralogical Magazin,* **74(1)**, 159-177 (2010)

Hydroxyapatite – enamel and dentine $Ca(2)_6Ca(1)_4(PO_4)_6(OH)_2$

ADT analysis on 3 enamel and 2 dentine crystals deliver best solutions for $P6_3$

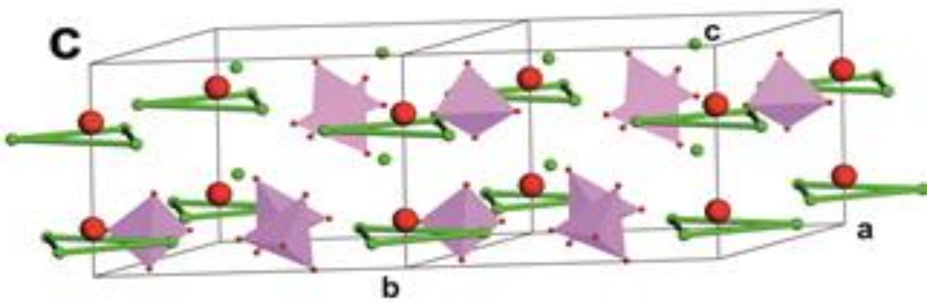

$P6_3$

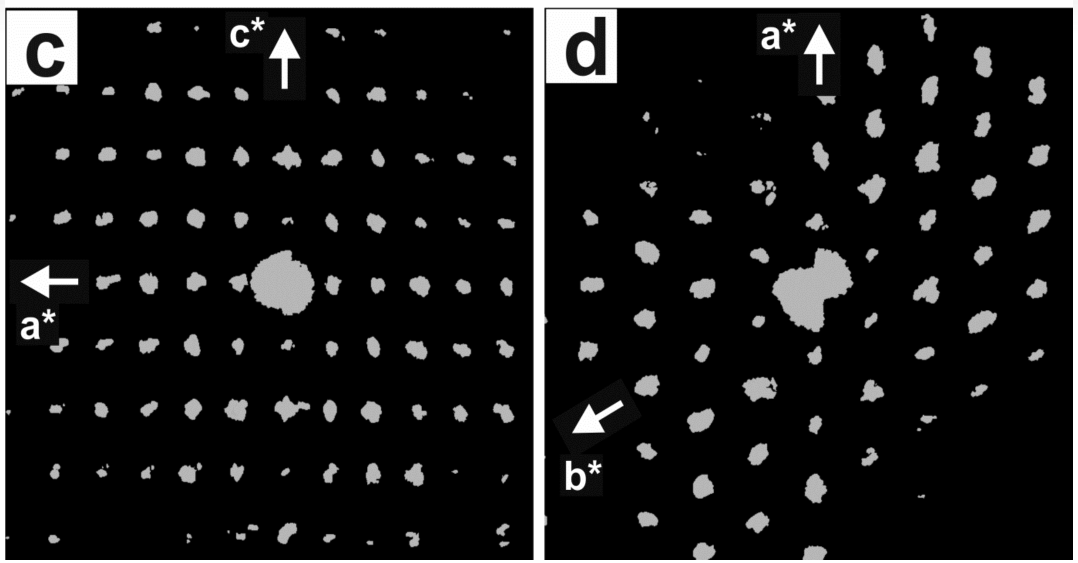

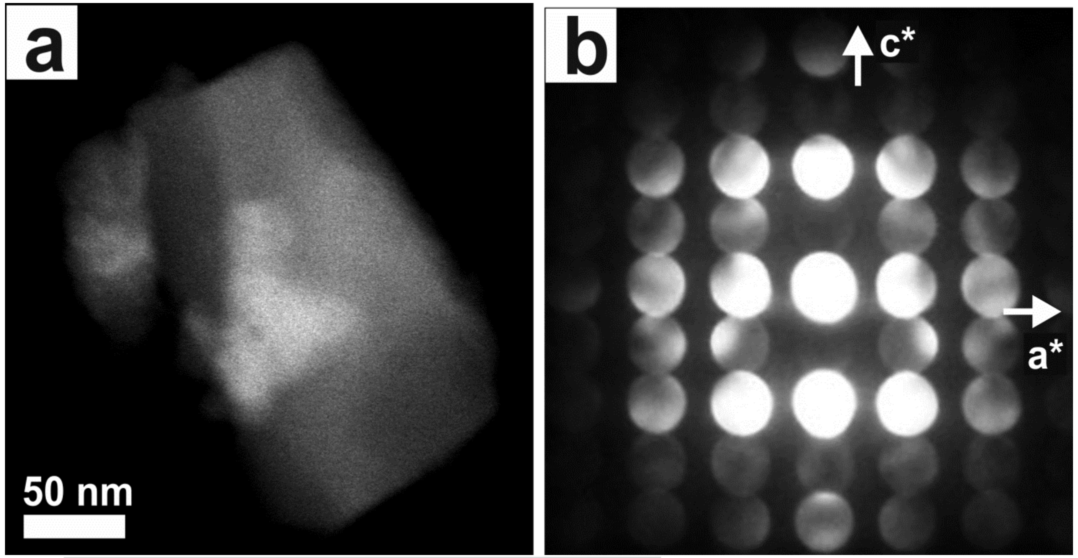

Contrast differences:
02-21 and 02-2-1
02-22 and 02-2-2

→ No mirror perpendicular to c

E. Mugnaioli, J. Reyes-Gasga, R. Garcia-García, U. Kolb, J. Hémmerlé, É. F. Brès, *Chem. Eur. J.* **20**, 6849 – 6852 (2014)

Bi-sulfate incrustations, oxidation of bismuthinite (Bi_2S_3) Alfenza mine, Italy

Monoclinic spacegroup *Pc* or $P2_1/c$; a=22.0, b=16.7, c=15.9 Å, β=102.9°, strong disorder along a*
→ Structure could not be solved

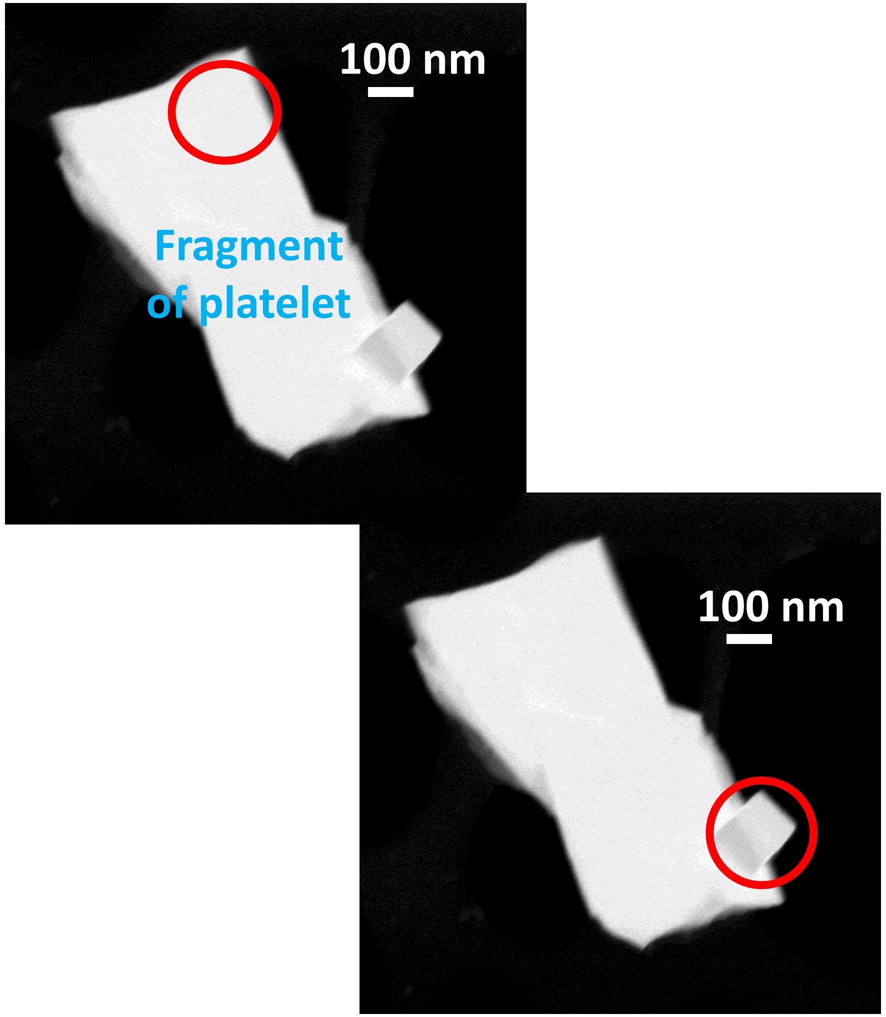

Hexagonal $P6_3mc$, *P*-62*c* or $P6_3/mmc$, a=9.6, c=15.3 Å

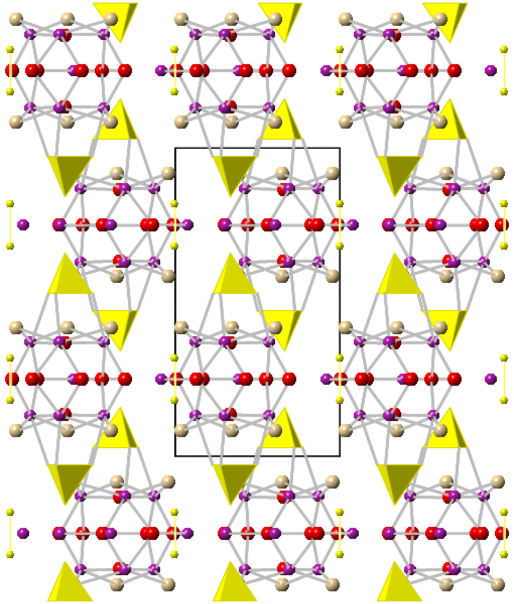

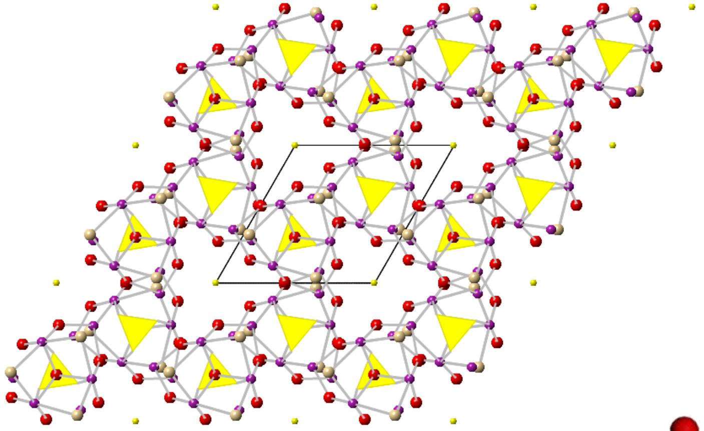

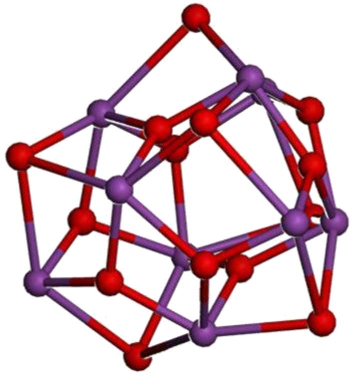

$Bi_{9-x}Te_x(OH)_6O_8$ clusters and SO_4 groups

EDX reveals only for this phase a small amount of Te

G. C. Capitani, E. Mugnaioli, J. Rius, P. Gentile,.T. Catelani, A. Lucotti, U. Kolb, *American Mineralogist*, **99(2-3)** 500-510 (2014)

Zeolite beta - stacking disorder visualized by ADT

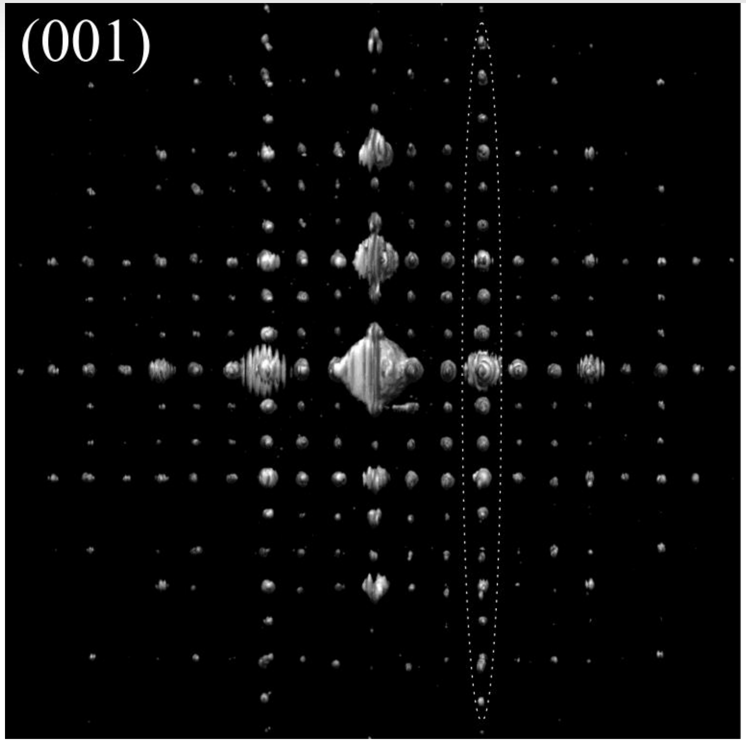

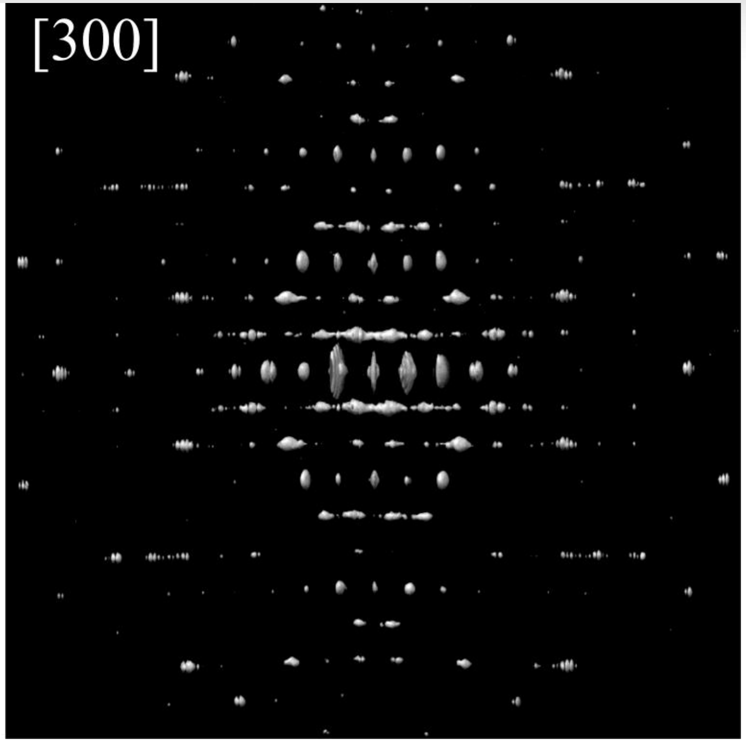

Polytype A:
P$4_1$22
a = 12.66 Å
c = 26.41 Å

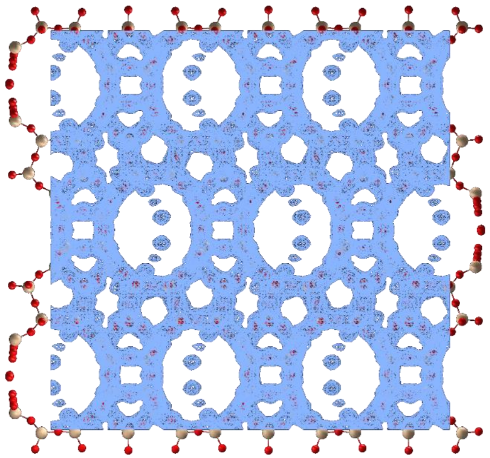

Polytype B:
*C*2/*c*
a = 17.90 Å, b = 17.92 Å
c = 26.41 Å´, β = 114,8°

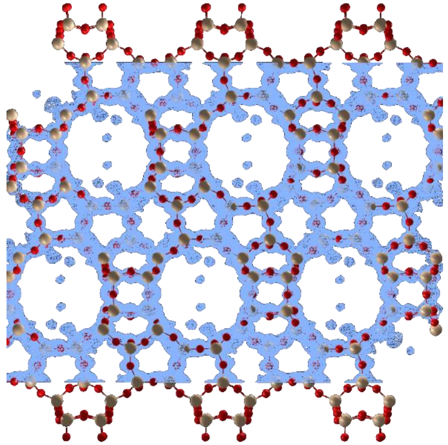

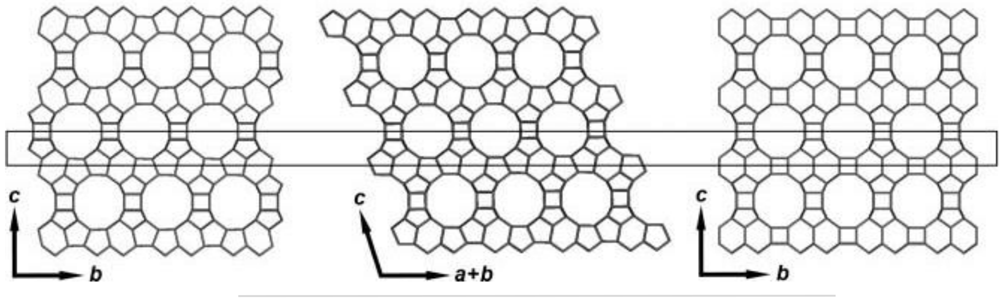

Vaterite – superstructure solved ab-initio by direct methods

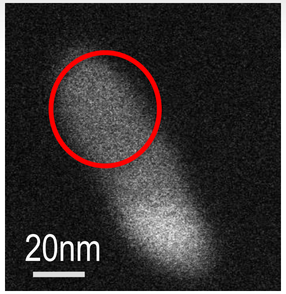

Space group C2/c

views down [010] and [103] (equivalent to [001] in the previous hexagonal structure models)

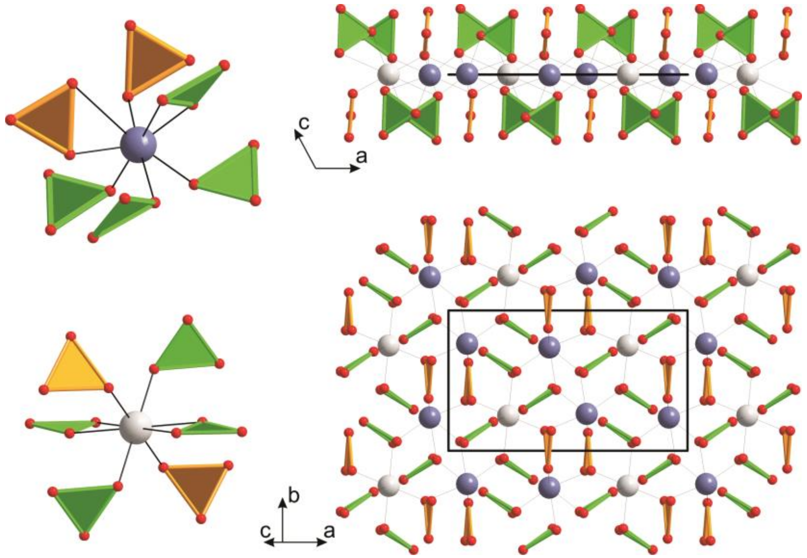

Structure explains all features observed in the Raman spectrum

Space group *C-1*

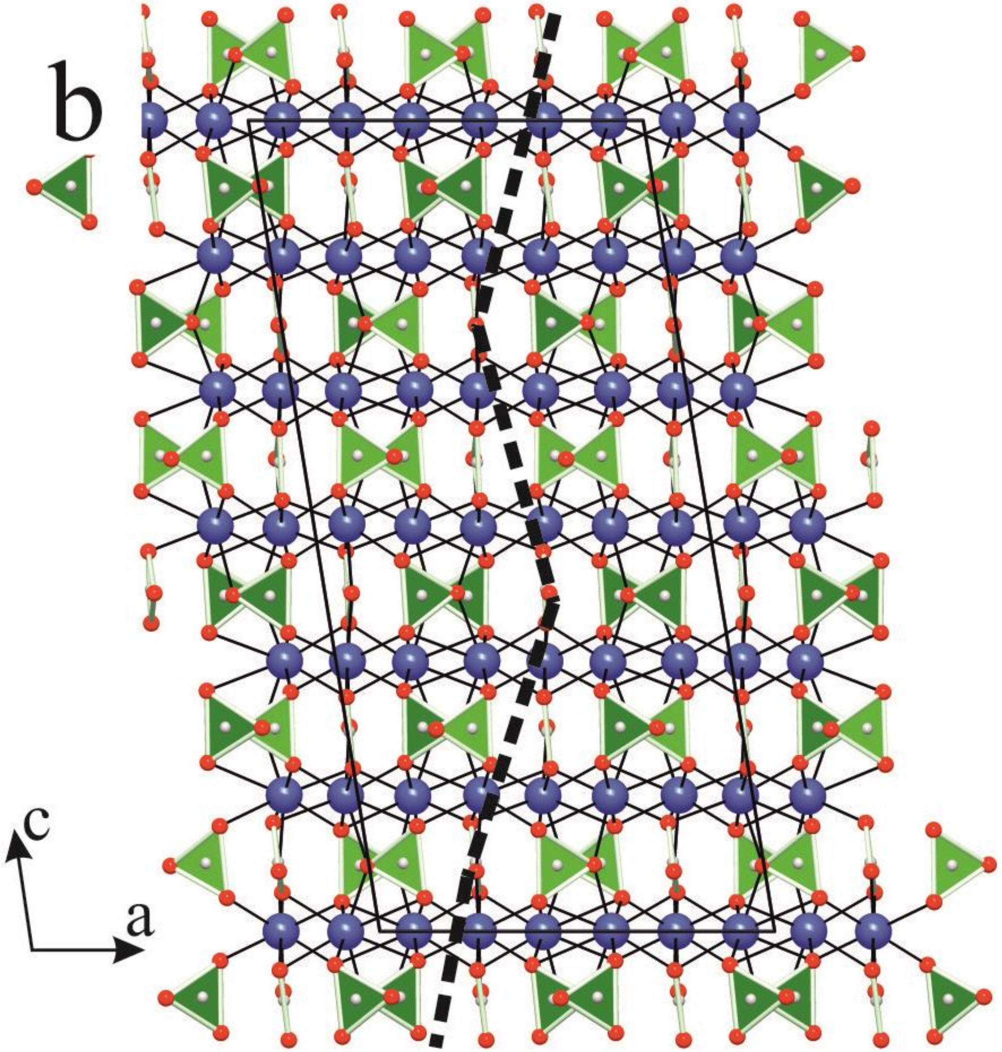

E. Mugnaioli, I. Andrusenko, T. Schüler, N. Loges, R. Dinnebier, M. Panthöfer, W. Tremel and U. Kolb, *Angewandte Chem.Int. Ed.*, **51(28)** 7041-7045 (2012)

Conclusion

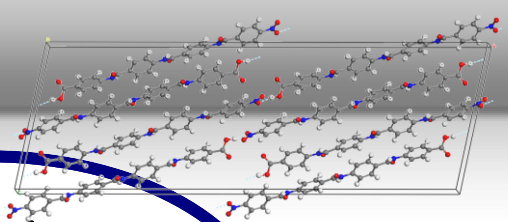

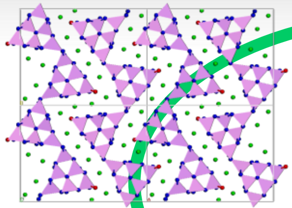

Phosphates:
SrP_3N_5O
$Ba_6Br_3P_{12}N_{17}O_9$

Organic-inorganic hybrids:
ECS-3, ECS-5

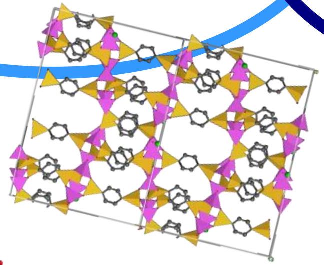

Organic:
Pharmaceuticals
Amides
Dyes

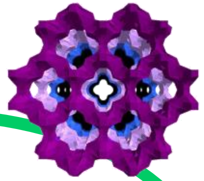

Zeolites:
ITQ-43, ITQ-45, ITQ-N
ZSM-5, ZSM-25,
Zeolite beta

Oxides:
$Na_2W_4O_{13}$
$Li_2Ti_3NiO_8$
$NaHTi_3O_7 \cdot H_2O$
$Na_2Ti_6O_{13}$

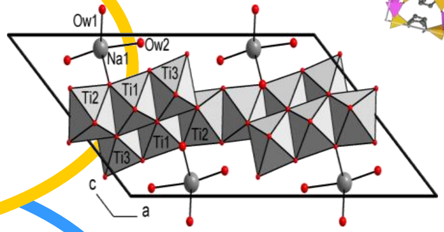

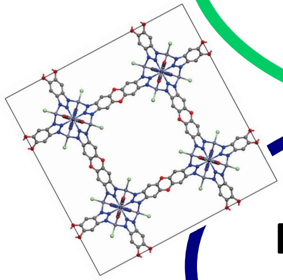

Metal Organic Frameworks (MOF):
MUF-4l
Bi(BTB)

Intermetallic nanophases:
Zn_8Sb_7

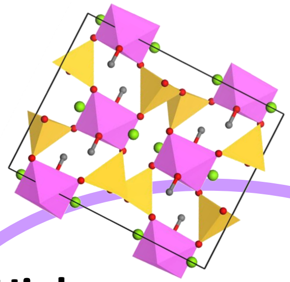

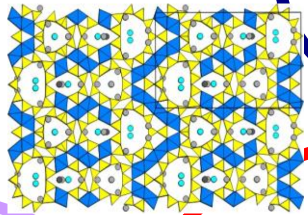

Ca-compounds:
Vaterite $CaCO_3$
$Ca_5Si_6O_{17} \cdot 5H_2O$
$Ca_5(PO_4)_3(OH)$

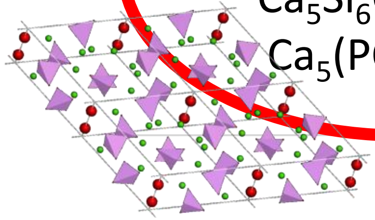

High pressure phases:
HP hydrous Al-pyroxene
$(Mg_2Al(OH)_2AlSiO_6)$

Minerals:
Sarrabusite
$(S_2)_{1+x}[Bi_{9-x}Te_x(OH)_6O_8(SO_4)_2]_2$
Charoite-90/96
Chukanovit
Cannonit

The group

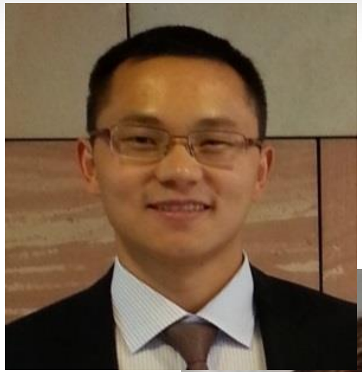
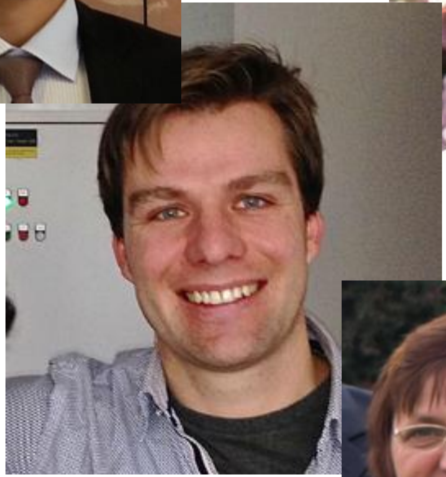


Photo: Dr. Peter Müller, MIT, Cambridge, MA

Tatiana Gorelik
Galina Matveeva
Bastian Barton
Yasar Krysiak
Haishuang Zhao

Enrico Mugnaioli
Andrew Stewart
Sebastian Schlitt
Iryna Andrusenko

Thank you for your attention

Financial Support:

Stiftung Rheinland-Pfalz Innovation
SFB 625
SPP 1415

TECHNISCHE UNIVERSITÄT DARMSTADT

JG|U
JOHANNES GUTENBERG UNIVERSITÄT MAINZ